İSTANBUL TECHNICAL UNIVERSITY ★ INSTITUTE OF SCIENCE AND TECHNOLOGY

A SECOND ORDER NEWTON METHOD FOR RECONSTUCTION OF PERFECTLY ELECTRIC CONDUCTING OBJECTS

Ph.D. Thesis by
Necmi Serkan Tezel

Department : Electronics and Communication Engineering

Programme : Electronics and Communication Engineering

APRIL 2010

İSTANBUL TECHNICAL UNIVERSITY ★ INSTITUTE OF SCIENCE AND TECHNOLOGY

A SECOND ORDER NEWTON METHOD FOR RECONSTUCTION OF PERFECTLY ELECTRIC CONDUCTING OBJECTS

Ph.D. Thesis by
Necmi Serkan Tezel
(504012044)

Date of submission : **12 May 2009**
Date of defence examination: **5 April 2010**

Supervisor (Chairman) : **Doç. Dr. Selçuk Paker (ITU)**
Members of the Examining Committee : **Doç. Dr. Cevdet Işık (ITU)**
Prof. Dr. Ercan Topuz (DU)
Prof.Dr. Filiz Güneş (YTU)
Prof.Dr. Selim Şeker (BU)

APRIL 2010

İSTANBUL TEKNİK ÜNİVERSİTESİ ★ FEN BİLİMLERİ ENSTİTÜSÜ

İKİNCİ DERECE NEWTON YÖNTEMİYLE MÜKEMMEL İLETKEN CİSİMLERİN ŞEKLİNİN BULUNMASI

DOKTORA TEZİ
Necmi Serkan TEZEL
(504012044)

Tezin Enstitüye Verildiği Tarih : 12 Mayıs 2009
Tezin Savunulduğu Tarih : 5 Nisan 2010

Tez Danışmanı : Doç. Dr. Selçuk PAKER (İTÜ)
Diğer Jüri Üyeleri : Prof. Dr. Filiz Güneş (YTÜ)
Prof. Dr. Selim ŞEKER (BÜ)
Doç.Dr. Cevdet Işık (ITÜ)
Prof.Dr. Ercan Topuz (DÜ)

NİSAN 2010

FOREWORD

I would like to express my deep appreciation and thanks for my advisor and Prof.Dr. Rainer Kress. This work is supported by ITU Institute of Science and Technology.

May 2009

Necmi Serkan Tezel

Electronics and Communication Department

TABLE OF CONTENTS

Page

ABBREVIATIONS

PEC **:** Perfectly Electrical Conductor

LIST OF TABLES

Page

LIST OF FIGURES

Page

A SECOND ORDER NEWTON METHOD FOR RECONSTRUCTION OF PERFECTLY ELECTRIC CONDUCTING OBJECTS

SUMMARY

Inverse scattering problems for time harmonic waves are of fundamental importance in applications such as radar and sonar, nondestructive evaluation, geophysical exploration, medical imaging and others. In principle, in these applications the wave scattered by an unknown object is measured at a number of discrete locations and information such as shape parameters, location parameters and electromagnetic parameters of the scatterer are extracted from these data.

In this study, a new second order Newton method for reconstructing the shape of a arbitrary cylindrical perfectly electrical conducting (PEC) scatterer from the measured far-field pattern for scattering of time harmonic plane waves is presented the first time in this thesis. This method extends a hybrid between regularized Newton iterations and decomposition methods. The main idea of our iterative method is to use Huygen's principle, i.e., represent the scattered field as a single-layer potential. Given an approximation for the boundary of the scatterer, this leads to an ill-posed integral equation of the first kind that is solved via Tikhonov regularization. Then, in a second order Taylor expansion, the PEC boundary condition is employed to update the boundary approximation. In an iterative procedure, these two steps are alternated until some stopping criterium is satisfied. Main advantages of method is that method does not need forward solver in each iteration step and needs less iteration than first order Newton method in order to obtain desired accuracy. Method can be easily extended for limited angular and near field measurements of scattered fields. Proposed method is described in detail and illustrated its feasibility through examples with exact and noisy data.

İKİNCİ DERECE NEWTON YÖNTEMİYLE MÜKEMMEL İLETKEN CİSİMLERİN ŞEKLİNİN BULUNMASI

ÖZET

Zamanda harmonik dalgaların ters saçılma problemi radar, sonar, tahribatsız değerlendirme, geofizik, tıbbi görüntüleme gibi uygulamalar için temel öneme sahiptir. Temel olarak, bu uygulamalarda bilinmeyen cisimden saçılan dalganın ayrık noktalarda ölçülmesiyle elde edilen data kullanılarak caçıcının şekil, konum, elektromagnetik parametreleri gibi özellikleri bulunur.

Bu çalışmada, düzlemsel bir dalga ile aydınlatılmış rastgele kesitli silindirik mükemmel iletken bir cisimden saçılan alanların uzak alan ölçümlerinden şeklinin bulunması yeni bir yöntem olan ikinci dereceden Newton metoduyla ilk kez bu tezde incelenmiştir. Bu yöntem Newton iterasyonu ve dekompozisyon methodunun daha gelişmiş bir şeklidir. Buradaki iteratif yöntemin ana fikri Huygen prensibini kullanmaktır yani saçılan alanı tek tabakalı bir potansiyelle ifade etmektir. Saçıcının alınan bir yaklaşıklığı için bu Tikhonov regülarizasyonuyla çözülebilen birinci dereceden ill-posed bir integral denklem elde edilir. Daha sonra, ikinci dereceden Taylor açılımıyla mükemmel iletken sınır koşulu sağlanacak şekilde cismin şekli değiştirilir. Iterasyon yönteminde bu iki adım belirlenmiş bir durma koşulu sağlanana kadar devam ettirilir. Bu yöntemin temel avantajları herbir iterasyonda düz probleminin çözümünün gerekmemesi ve birinci dereceden Newton yöntemine göre arzulana bir doğruluğa ulaşmak için daha az iterasyon gerektirmesidir. Önerilen yöntem yakın alan ve sınırlı alan ölçümlerinin saçılan alan olarak kullanılması durumuna kolayca geliştirilebilir. Bu yöntem detaylı olarak incelenecek ve tam ve gürültülü datalar için uygulanabilirliği örneklerle gösterilmiştir.

1. INTRODUCTION

Inverse scattering problems for time harmonic waves are of fundamental importance in applications such as radar and sonar, nondestructive evaluation, geophysical exploration, medical imaging and others. In principle, in these applications the wave scattered by an unknown object is measured at a number of discrete locations and information such as shape parameters, location parameters and electromagnetic parameters of the scatterer are extracted from these data. As opposed to classical techniques of imaging such as computerized tomography that is based on the fact that x-rays travel along straight lines, inverse scattering problems take into account that the propagation of acoustic, electromagnetic and elastic waves have to be modeled by a wave equation. This means that inverse scattering requires a nonlinear model, whereas inverse tomography is a linear approximation of inverse scattering problems.

1.1 Literature

The first attempt to reconstruct the shape of a perfectly electric conducting (PEC) obstacle from a knowledge of the far field pattern in a manner acknowledging the nonlinear and ill-posed nature of the problem was made by Roger in 1981 [1]. Roger considered the scattering of a plane wave propagating in a fixed direction by a two dimensional PEC scatterer parameterized in the form $x = r(\hat{x})\hat{x}$, where $r(\hat{x}) = |x|$, and then solved the nonlinear operator equation $F(r) = u_\infty$ by Newton's method, where the Frechet derivative of F was inverted using Tikhonov regularization. A characterization and rigorous proof of the existence of the Frechet derivative of F was subsequently established by Kirsch [2] and Potthast [3] (see also [4], [5] and [6]). An alternative approach to solving the inverse scattering problem for a PEC obstacle was proposed by Kirsch and Kress [7] (see also [4]), who broke up the inverse scattering problem into two parts. The first part deals with the ill-posedness by constructing the scattered field us from the far field pattern u_∞ by representing

u^s in the form of a surface potential defined on a surface known a priori to be contained in the unknown scatterer D. The second part then deals with the nonlinearity of the problem by determining the unknown boundary of the scatterer as the location of the zeros of the total field $u = u^i + u^s$ where u^i is again a plane wave propagating in a fixed direction. An advantage of this approach is that the cost functional of the nonlinear part of the problem has a particularly simple structure from which the Frechet derivative is easily computed. Related methods have also been proposed by Angell, Jiang and Kleinman [8], Colton and Monk [9], Misici and Zirilli [10], and Potthast [11]. Detailed literature survey can be found in Colton and Monk [12].

In this study, we are interested in shape reconstruction of PEC obstacles from measurements of the far field pattern by using a new variant of a second order Newton method given in [13]. This method extends a hybrid between regularized Newton iterations and decomposition methods that has been suggested and analyzed in a number of papers by Kress and Serranho [14, 15, 16, 17, 18] and has some features in common with the second degree method for ill-posed nonlinear problems as considered by Hettlich and Rundell [19]. As a major advantage, this iterative algorithm does not require a forward solver at each iteration step. Our approach extends a corresponding first order Newton method as suggested and analyzed by Kress and Serranho for shape reconstruction for sound soft [14, 17] and sound hard obstacles [16] and for the reconstruction of both the shape and the boundary impedance [18]. Although, in the present paper the obstacle is assumed to be smooth, since the approach of Kress and Serranho has also been extended to cracks [15] we expect that our method also can be carried over to this case.

To some extend our approach is related to a method that has been suggested and investigated more recently by Cayören et al [20]. The main difference is that in [20] the curve on which the Taylor expansion is employed remains fixed throughout the algorithm and that, in order to compensate for this, higher order Taylor expansions are used. This also implies that the method of Cayören et al only works properly when the approximating curve for the Taylor expansion is not too far away from the actual boundary to be reconstructed, whereas our method is more flexible with this respect through its alternating nature.

The idea of our algorithm differs from the traditional regularized Newton type iterations for the inverse obstacle scattering problem. The latter approach is based on the observation that the solution to the direct scattering problem with a fixed incident plane wave u^i defines an operator $A:\partial D \to u_\infty$ that maps the boundary ∂D of the scatterer D onto the far field pattern u_∞ of the scattered wave. In terms of this operator, given a far field pattern u_∞, the inverse problem just consists in solving the nonlinear and ill-posed operator equation $A(\partial D) = u_\infty$ for the unknown surface ∂D which, for example, can be done via regularized Newton iterations as has been suggested for the first time by Roger [1]. For details on this approach we refer to [4]. Numerical examples in three dimensions have been more recently reported by Farhat et al [21] and by Harbrecht and Hohage [22]. A related second order Newton scheme has been considered by Hettlich and Rundell [19]. As opposed to our method, the numerical implementation of Newton type iterations for the solution of $A(\partial D) = u_\infty$ requires the solution of the forward problems to evaluate *A* and its derivatives for the current approximation of ∂D in each iteration step. Main scientific contribution of our second order Newton method given in [13] is that this method needs less iteration than known first order approach [14] and more robust against noisy data. Exploiting the fact that field satisfies Helmholtz equation outside the scatterer, the second order normal derivative of the field on the estimated scatterer can be obtained analytically which provides that each iteration of second order and first order Newton needs approximately same CPU time.

Proposed new second order Newton reconstruction method can be extended straightforwardly for multi illumination cases. In this case, object is illuminated by multi plane waves separately each having different propagation direction. Scattered data is obtained on unit circle Ω for each illumination. Since more data is available for this case, multi illuminations provide better reconstruction than single illumination especially in shadow region of object. Moreover, it is also possible to use proposed reconstruction method for any excitation as an incident field such as line source instead of plane wave.

Proposed method can be extended for reconstruction of perfectly electric conducting (PEC) objects located on known domain by using the fundamental solution of Helmholtz equation on known domain and its far field pattern and using the incident field as field in the absence of the PEC object. Fundamental solution of Helmoltz

equation on known domain $\phi(x, y)$ simply is total field on x if line source located on y. This is well known direct scattering problem. Therefore, $\phi(x, y)$ can be obtained straightforwardly. Field in the absence of the PEC object can also be obtained via direct scattering problem for plane wave excitation. This approach have been applied for reconstruction of objects buried in a arbitrary shaped cylinder by using second order method in [23]. Shape reconstruction of the PEC object buried in dielectric half space by first order Newton method is given in [24]. The considered problem given in [24] can be applied for detection of mines, pipes, tunnels etc..Because of the nature of the this problem, scattered field data can be obtained only upper half space. Fundemantal solution of Helmoltz equation on this domain can be obtained by integral representation on complex plane given in [24,25]. It is also straightforwardly possible to extend the method in [24] for detection of PEC objects buried in rough surface by using the Green's function of rough surface given in [26]. Time dependence is assumed $e^{-i\omega t}$ and omitted throughout the thesis.

1.2. Definition of the Problem

Given an open bounded obstacle $D \subset R^2$ with an unbounded and connected complement and a smooth boundary ∂D and an incident field u^i as depicted fig. 1, the direct scattering problem consists of finding the total field $u = u^i + u^s$ as the sum of the known incident field u^i and the scattered field u^s, such that the Helmholtz equation

$$\Delta u + k^2 u = 0, \quad in \ R^2 / D \tag{1.1}$$

and PEC boundary condition,

$$u = 0 \quad on \ \partial D \tag{1.2}$$

are fulfilled and the scattered wave u^s satisfies the Sommerfeld radiation condition

$$\lim_{r\to\infty} \sqrt{r}\left(\frac{\partial u^s}{\partial r} - iku^s\right) = 0, \quad r = |x| \tag{1.3}$$

uniformly with respect to all directions. The latter ensures an asymptotic behavior of the scattered wave of the form

$$u^s(x) = \frac{e^{ik|x|}}{\sqrt{|x|}}\left\{u_\infty(\hat{x}) + 0\left(\frac{1}{|x|}\right)\right\}, \quad |x| \to \infty \tag{1.4}$$

uniformly in all directions with the far field pattern u_∞ defined on the unit circle Ω.

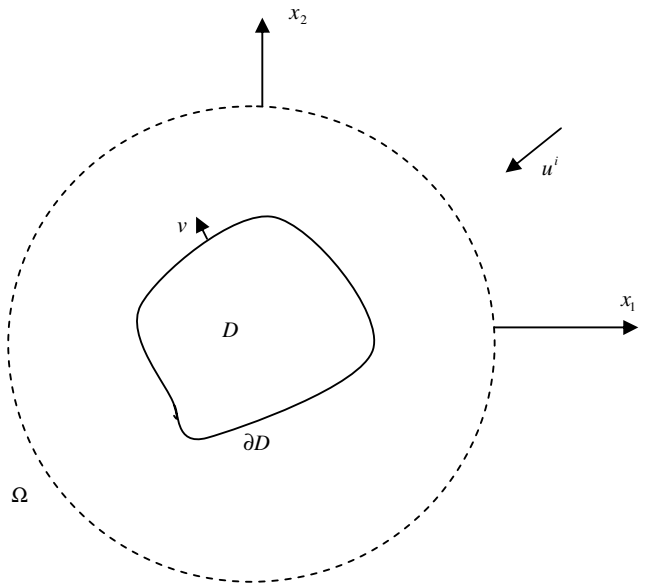

Figure 1.1 : Geometry of the problem.

The inverse scattering problem we are interested in is to determine the shape of the scatterer D from a knowledge of the far field pattern u_∞ for one or several incident plane waves $u^i = e^{ikx.d}$ with incident direction $d \in \Omega$. We note that the inverse scattering problem we have just formulated is ill-posed in the sense that the determination of ∂D does not depend continuously on the measured far field data in any reasonable norm. This issue of ill-posedness will be handled using Tikhonov regularization in our reconstruction algorithm.

This algorithm starts from Green's representation formula for the scattered wave on the Γ_0 initial estimate of the boundary ∂D as

$$u^s(x) = -\frac{i}{4}\int_{\Gamma_0} \frac{\partial u}{\partial v}(y) H_0^{(1)}(k|x-y|) ds(y), \quad x \in R^2 \setminus \overline{\Gamma}_0 \tag{1.5}$$

and its far field pattern

$$u_\infty(\hat{x}) = -\frac{e^{i\pi/4}}{\sqrt{8\pi k}} \int_{\Gamma_0} \frac{\partial u}{\partial \nu}(y) e^{-ik\hat{x}.y} ds(y), \quad \hat{x} \in \Omega \tag{1.6}$$

that is, Huygen's principle (see Theorem 3.12 in [9]). Here, $H_0^{(1)}$ denotes the Hankel function of order zero and of the first kind and ν is the outward unit normal to Γ_0. We view (1.6) as the data equation in terms of the measured far field pattern u_∞. Given an approximation for the boundary ∂D, we solve (1.6) for the unknown flux $\varphi := -\partial u / \partial \nu$. Then we insert the scattered wave (1.5) into the boundary condition (1.2) and consider this as the field equation which we solve for updating the approximation for ∂D. This is achieved via a Taylor expansion up to order two for u along the normal direction and solving the quadratic equation for the update function. In an obvious way, these two steps are iterated until an appropriate stopping criterium is satisfied. This method decomposes the inverse scattering problem into ill-posed and non-linear part and deals with each part of the problem separately. This provides that method does not need forward solver in each iteration step. On the other hand, another advantage of this approach is that the cost functional of the nonlinear part of the problem has a particularly simple structure from which the first and second order Frechet derivatives are easily and analytically computed by exploiting the fact that field satisfies Heltmoltz equation outside the object [13]. This provides each iteration of second order and first order Newton needs approximately same CPU time.

2. DIRECT SCATTERING BY NYSTRÖM METHOD

In this section, Electromagnetic scattering from PEC object is given by Nyström method. Nyström method have exponential converge property therefore it is very computational effective. Although, direct scattering from two dimensional objects are well known and straightforward, it has be considered in order to produce data and implement Newton method.

PEC object with boundary ∂D is located in medium whose wave number is k. This object is illuminated by x_3 polarized plane wave with propagation direction d as $u^i(x) = e^{ikx.d}$. Since the problem is homogeneous with respect to x_3 axis, scattered field is also x_3 polarized and problem reduces scalar problem in $x \in R^2$ such that total field satisfies Helmholtz equation,

$$\Delta u + k^2 u = 0, \quad x \in R^2 \setminus \overline{\mathrm{D}} \tag{2.1}$$

with PEC or Dirichlet boundary condition as

$$u(x) = u^i(x) + u^s(x) = 0, \quad x \in \partial D \tag{2.2}$$

and scattered field satisfies radiation condition as

$$\lim_{r \to \infty} \sqrt{r} \left(\frac{\partial u^s}{\partial r} - iku^s \right) = 0, \quad r = |x| \tag{2.3}$$

uniformly with respect to all directions. The latter ensures an asymptotic behavior of the scattered wave of the form

$$u^s(x) = \frac{e^{ik|x|}}{\sqrt{|x|}} \left\{ u_\infty(\hat{x}) + 0\left(\frac{1}{|x|} \right) \right\}, \quad |x| \to \infty \tag{2.4}$$

uniformly in all directions with the far field pattern u_∞ defined on the unit circle Ω. Direct scattering problem is to find unknown scattered field u^s for given boundary ∂D and incident field u^i.

2.1 Solution of Direct Scattering Problem by Single-Layer Potantial

if k^2 is not a Dirichlet eigenvalue for the negative Laplacian in the interior of ∂D, scattered field, which satifies (2.1) and (2.3), can be expressed by single layer potential by [4]

$$u^s(x) = \int_{\partial D} \varphi(y)\phi(x,y)ds(y), \quad x \in R^2 \setminus \overline{\mathrm{D}} \tag{2.5}$$

where $\phi(x,y)$ is fundamental solution of Helmholtz equation in R^2, in other words Green's function of the medium given by [4]

$$\phi(x,y) = \frac{i}{4} H_0^{(1)}(k|x-y|) \tag{2.6}$$

where $H_0^{(1)}(.)$ is Hankel function of first kind and order zero. Substituting (2.4) into (2.2), one gets integral equation defined on the boundary ∂D as

$$\int_{\partial D} \varphi(y)\phi(x,y)ds(y) = -u^i(x), \quad x \in \partial D \tag{2.7}$$

Let's represent the boundary ∂D of the object by parameterization as

$$\partial D = \{z(t) = (x_1(t), x_2(t)),\ t \in [0, 2\pi)\} \tag{2.8}$$

In this case, integral equation in (2.7) can be given by

$$\int_0^{2\pi} \varphi(z(\tau))M(t,\tau)|z'(\tau)|d\tau = -u^i(z(t)), \quad t \in [0, 2\pi) \tag{2.9}$$

Kernel of the integal equation (2.9) is expressed by

$$M(t,\tau) = \frac{i}{4} H_0^{(1)}(k|z(t) - z(\tau)|) \tag{2.10}$$

and can be decomposed as

$$M(t,\tau) = M_1(t,\tau)\ln\left(4\sin^2\left(\frac{t-\tau}{2}\right)\right) + M_2(t,\tau) \tag{2.11}$$

where

$$M_1(t,\tau) = -\frac{1}{4\pi} J_0(k|z(t) - z(\tau)|) \tag{2.12}$$

$$M_2(t,\tau) = M(t,\tau) - M_1(t,\tau)\ln\left(\sin^2(\frac{t-\tau}{2})\right) \tag{2.13}$$

are analytic with diagonal terms

$$M_1(t,t) = -\frac{1}{4\pi} \tag{2.14}$$

$$M_2(t,t) = \frac{i}{4} - \frac{C}{2\pi} - \frac{1}{2\pi}\ln\frac{k|x'(t)|}{2} \tag{2.15}$$

where $C = 0.577215...$ is Euler constant.

Substituting (2.11) into (2.9), one gets

$$\int_0^{2\pi} \varphi(z(\tau))\left(M_1(t,\tau)\ln\left(4\sin^2(\frac{t-\tau}{2})\right) + M_2(t,\tau)\right)|z'(\tau)|d\tau = -u^i(t) \tag{2.16}$$

Using the equation [4],

$$\int_0^{2\pi} \ln\left(4\sin^2(\frac{t-\tau}{2})\right) f(\tau) \approx \sum_{j=0}^{2N-1} R_j^{(N)}(t) f(t_j^{(N)}) \tag{2.17}$$

where N is discretization number of integral equation and

$$t_j^{(N)} = \frac{j\pi}{N} \tag{2.17}$$

$$R_j^{(n)}(t) = -\frac{2\pi}{N}\sum_{m=1}^{N-1}\frac{1}{m}\cos m(t - t_j^{(N)}) - \frac{\pi}{N^2}\cos(N(t - t_j^{(N)})) \tag{2.18}$$

In addition, we use the trapezoidal rule

$$\int_0^{2\pi} f(\tau)d\tau = \frac{\pi}{N}\sum_{j=0}^{2N-1} f(t_j^{(N)}) \tag{2.19}$$

Substituting (2.19) and (2.16) into (2.15), one gets

$$\sum_{j=0}^{2N-1}\varphi(t_j^{(N)})\left\{R_j^{(N)}(t)M_1(t,t_j^{(N)})+\frac{\pi}{N}M_2(t,t_j^{(N)})\right\}\left|z'(t_j^{(N)})\right|=-u^i(t) \qquad \textbf{(2.20)}$$

(2.20) is evaluated at collocation points called by $t_k=0,1,...2N-1$, one gets linear equation [4] where

$$\sum_{j=0}^{2N-1}\varphi(t_j^{(N)})\left\{R_{|k-j|}^{(N)}M_1(t_k^{(N)},t_j^{(N)})+\frac{\pi}{N}M_2(t_k^{(N)},t_j^{(N)})\right\}\left|z'(t_j^{(N)})\right|=-u^i(t_k^{(N)}) \qquad \textbf{(2.21)}$$

$k=0,1,.....,2N-1$

where

$$R_j^{(N)}=R_j^{(N)}(0)=-\frac{2\pi}{N}\sum_{m=1}^{N-1}\frac{1}{m}\cos\frac{mj\pi}{N}+\frac{(-1)^j\pi}{N^2} \qquad \textbf{(2.22)}$$

that can be solved straightforwardly. After solution of (2.21), scattered field can be calculated by (2.4). By using large argument approximation of Hankel functions, one obtains scattered field for $|x|\to\infty$ as

$$u(x)=\frac{e^{i\pi/4}}{\sqrt{8\pi k}}\frac{e^{ik|x|}}{\sqrt{|x|}}\int_{\partial D}\varphi(y)e^{-ik\hat{x}.y}ds(y),\quad \hat{x}=x/|x|,\quad |x|\to\infty \qquad \textbf{(2.23)}$$

Comparing (2.23) and (2.5), one obtains far field pattern by

$$u_\infty(\hat{x})=\frac{e^{i\pi/4}}{\sqrt{8\pi k}}\int_{\partial D}\varphi(y)e^{-ik\hat{x}.y}ds(y),\quad \hat{x}\in\Omega \qquad \textbf{(2.24)}$$

where Ω is unit circle. We again outlined the fact that proposed single layer approach can be applied for solution of direct scattering problem, if k^2 is not a Dirichlet eigenvalue for the negative Laplacian in the interior of ∂D. Otherwise, combined single and double layer representation of scattered field is used.

2.1 Solution of Direct Scattering Problem by Combined Single and Double Layer Potantials

Scattered field, which satifies (2.1) and (2.3), can also be expressed by combined single and double layer potential by [4]

$$u^s(x)=\int_{\partial D}\left\{\frac{\partial\phi(\mathrm{x},\mathrm{y})}{\partial \mathrm{v}(\mathrm{y})}-i\eta\phi(x,y)\right\}\varphi(y)ds(y),\quad x\in R^2\setminus\overline{\mathrm{D}} \qquad \textbf{(2.25)}$$

with unknown density φ and some real coupling parameter η. Substituting (2.25) into (2.2), and using jump relation related to single and double layer potantials, one obtains boundary integral equation given by

$$\int_{\partial D}\left\{\frac{\partial\phi(\mathrm{x},\mathrm{y})}{\partial \mathrm{v}(\mathrm{y})}-i\eta\phi(x,y)\right\}\varphi(y)ds(y)+\frac{\varphi(x)}{2}=-u^{i}(x),\quad x\in\partial D \tag{2.26}$$

Substituting (2.6) into (2.26), (2.26) can be expressed by

$$\frac{i}{4}\int_{\partial D}\left\{\frac{k\hat{y}(y).\{x-y\}}{|x-y|}H_1^{(1)}(k|x-y|)-i\eta H_0^{(1)}(k|x-y|\right\}\varphi(y)ds(y)+\frac{\varphi(x)}{2}=-u^{i}(x),\quad x\in\partial D \tag{2.27}$$

if parametric representation of boundary ∂D is given by (2.8), (2.27) can be given by

$$\int_{0}^{2\pi}(L(t,\tau)-i\eta M(t,\tau)|z'(\tau)|)d\tau \tag{2.28}$$

where $M(t,\tau)$ is given by (2.10) . Since normal vectoris espressed as $\hat{v}(t)=(x_2'(t),-x_1'(t))/|z'(t)|$, $L(t,\tau)$ is

$$L(t,\tau)=\frac{ik}{4}\frac{(x_2'(\tau).(x_1'(t)-x_1'(\tau))-x_1'(\tau).(x_2'(t)-x_2'(\tau))}{|z(t)-z(\tau)|}H_1^{(1)}(k|z(t)-z(\tau)|) \tag{2.29}$$

and can be decomposed as,

$$L(t,\tau)=L_1(t,\tau)\ln\left(4\sin^2\frac{t-\tau}{2}\right)+L_2(t,\tau) \tag{2.30}$$

where

$$L_1(t,\tau)=-\frac{k}{4\pi}\frac{(x_2'(\tau).(x_1'(t)-x_1'(\tau))-x_1'(\tau).(x_2'(t)-x_2'(\tau))}{|z(t)-z(\tau)|}J_1(k|z(t)-z(\tau)|) \tag{2.31}$$

$$L_2(t,\tau)=L(t,\tau)-L_1(t,\tau)\ln\left(4\sin^2\frac{t-\tau}{2}\right) \tag{2.32}$$

turn out to be analytic with the diagonal terms

$$L_1(t,t)=0 \tag{2.33}$$

$$L_2(t,t)=\frac{1}{4\pi}\frac{x_1''(t)x_2'(t)-x_2''(t)x_1'(t)}{|z'(t)|} \tag{2.34}$$

Using the (2.17) and (2.18) again, we get,

$$\sum_{j=0}^{2N-1}\varphi(t_j^{(N)})\Big\{R_j^{(N)}(t)(-i\eta M_1(t,t_j^{(N)})\left|z'(t_j^{(N)})\right|+L_1(t,t_j^{(N)}))$$
$$+\frac{\pi}{N}(-i\eta M_2(t,t_j^{(N)})\left|z'(t_j^{(N)})\right|+L_2(t,t_j^{(N)})\Big\}+\frac{\varphi(t)}{2}=-u^i(t) \quad \textbf{(2.35)}$$

and evaluating (2.35) is evaluated at collocation points called by $t_k = 0,1,...2N-1$, one gets linear equation

$$\sum_{j=0}^{2N-1}\varphi(t_j^{(N)})\Big\{R_{|j-k|}^{(N)}(t_k)(-i\eta M_1(t_k,t_j^{(N)})\left|z'(t_j^{(N)})\right|+L_1(t_k,t_j^{(N)}))$$
$$+\frac{\pi}{N}(-i\eta M_2(t_k,t_j^{(N)})\left|z'(t_j^{(N)})\right|+L_2(t_k,t_j^{(N)})\Big\}+\frac{\varphi(t_k)}{2}=-u^i(t_k) \quad \textbf{(2.36)}$$

$k = 0.1,..2N-1$

that is linear equation with 2N equation and 2N unknown which can be solved straightforwardly. After solving (2.36), scattered field can be obtained through (2.25). Far field pattern of (2.25) can be obtained as

$$\frac{e^{-i\pi/4}}{\sqrt{8\pi k}}\int_{\partial D}\{\eta-k\hat{v}(y).\hat{x}\}e^{-ik\hat{x}.y}\varphi(y)ds(y) \quad \textbf{(2.37)}$$

3. NEWTON METHOD FOR RECONSTRUCTION OF BOUNDARY

3.1 A First Order Newton Method for Reconstruction of Boundary

Object with boundary ∂D is illuminated by plane wave $u^i = e^{ikx.d}$ with propagation direction $d \in \Omega$. Far field pattern u_∞ of the object is obtained on Ω. Our problem is to find ∂D through measurements of far field pattern $u_\infty(\hat{x}), \hat{x} \in \Omega$.

Since we assume the boundary ∂D to be smooth, i.e., analytic, the scattered wave can be extended as solution to the Helmholtz equation across the boundary into a neighbourhood of ∂D. We now assume that an initial estimate Γ_0 for the boundary of the scatterer D is at our disposal such that this extension of u^s is defined in the closed exterior of Γ_0. Further we assume that k^2 is not a Dirichlet eigenvalue for the negative Laplacian in the interior of Γ_0. Then the scattered field can be expressed as a single-layer potential

$$u^s(x) = \frac{i}{4}\int_{\Gamma_0} \varphi(y) H_0^{(1)}(k|x-y|) ds(y), \quad x \in R^2 \setminus \Gamma_0 \tag{3.1}$$

for all x in the exterior of Γ_0 and a uniquely determined density $\varphi \in L^2(\Gamma_0)$ [4] Passing to the far field in (3.1) we obtain

$$\frac{e^{i\pi/4}}{\sqrt{8\pi k}}\int_{\Gamma_0} \varphi(y) e^{-ik\hat{x}.y} ds(y) = u_\infty(\hat{x}), \quad \hat{x} \in \Omega \tag{3.2}$$

as an integral equation of the first kind for the unknown density φ. Due to its analytic kernel, this integral equation is severely ill-posed. However, the operator $S_\infty : L^2(\Gamma_0) \to L^2(\Omega)$ defined by

$$(S_\infty \varphi)(\hat{x}) := \frac{e^{i\pi/4}}{\sqrt{8\pi k}}\int_{\Gamma_0} \varphi(y) e^{-ik\hat{x}.y} ds(y), \quad \hat{x} \in \Omega \tag{3.3}$$

is known to be injective and have dense range (see Theorem 5.17 in [4]). Therefore, Tikhonov regularization can be applied for a stable approximate solution of (3.2), that is, the ill-posed equation (3.2) is replaced by

$$\alpha\varphi_a + S_\infty^* S_\infty \varphi_\alpha = S_\infty^* u_\infty \qquad \textbf{(3.4a)}$$

with some positive regularization parameter α and the adjoint S_∞^* of S_∞ given by

$$(S_\infty^*\varphi)(\hat{x}) := \frac{e^{-i\pi/4}}{\sqrt{8\pi k}} \int_\Omega u_\infty(\hat{x}) e^{ik\hat{x}.y} ds(\hat{x}), \quad \hat{x} \in \Omega \qquad \textbf{(3.4b)}$$

For the further description of the reconstruction scheme we represent the curve Γ_0 by a regular parameterization

$$\Gamma_0 = \{z_0(t) : t \in [0,2\pi)\} \qquad \textbf{(3.5)}$$

with a periodic function $z_0 : R \to R^2$.

If far field data is obtained M discrete points on Ω called as $\hat{x}_m, m = 1,2...M$, and boundary Γ_0 with parametric representation given by $z_0(t), \quad t \in [0,2\pi)$ is discretized by 2N collocation points. Therefore (3.2) expressed by

$$\frac{e^{i\pi/4}}{\sqrt{8\pi k}} \frac{\pi}{N} \sum_{n=0}^{2N-1} \varphi(z(t_n)) e^{-ik\hat{x}_m . z(t_n)} \left| z_0'(t_n) \right| = u_\infty(\hat{x}_m), \quad m = 1,2...M \qquad \textbf{(3.6)}$$

that is linear equation system with M equation and 2N unknown is given by

$$S_\infty^{(MN)} \varphi = u_\infty^{(M)} \qquad \textbf{(3.7)}$$

with $S_\infty^{(MN)}$ matrix whose elements given by

$$s_{mn} = \frac{e^{i\pi/4}}{\sqrt{8\pi k}} \frac{\pi}{N} e^{-ik\hat{x}_m . z(t_n)} \left| z_0'(t_n) \right| \qquad \textbf{(3.8)}$$

Adjoint operator of far field pattern given by $S_\infty^* = S_\infty^{(MN)^H}$ that is Hermitian of $S_\infty^{(MN)}$.Therefore, Tikhonov regularized solution is given by

$$\varphi_\alpha = (\alpha I^{(NN)} + S_\infty^{(MN)^H} S_\infty^{(MN)})^{-1} S_\infty^{(MN)^H} u_\infty^{(M)} \qquad \textbf{(3.9)}$$

Searching the location where the boundary condition (1.2) is satisfied we approximate the total field u by the Taylor formula of order one with respect to the normal direction at Γ_0. For this we try to update in the form

$$\Gamma_1 = \{z_0(t) + h(t)v_0(t) : t \in [0,2\pi)\} \tag{3.10}$$

where v_0 denotes the outward normal vector to Γ_0 and h : IR → IR is a sufficiently small 2π periodic function. The normal vector can be expressed through the parameterization (3.5) via

$$v_0(t) = \frac{[z_0'(t)]^{\perp}}{|z_0'(t)|} \tag{3.11}$$

where for any vector $a = (a_1, a_2)$, we set $a^{\perp} = (a_2, -a_1)$. Then the first order Taylor formula requires the update function h to satisfy [13]

$$u \circ z_0 + \frac{\partial u}{\partial v} \circ z_0 h_0 = 0 \tag{3.12}$$

Once the single layer density φ is known from (3.9), the values u and $\partial u / \partial v$ of the total field on Γ_0 can be obtained through the jump relations for the single-layer potential [13], that is, by

$$u(x) = u^i(x) + \frac{i}{4}\int_{\Gamma_0} \varphi_\alpha(y) H_0^{(1)}(k|x-y|) ds(y) \tag{3.13}$$

and

$$\begin{aligned} \frac{\partial u}{\partial v}(x) &= \frac{\partial u^i}{\partial v}(x) + \frac{i}{4}\int_{\Gamma_0} \varphi_\alpha(y) \frac{\partial H_0^{(1)}(k|x-y|)}{\partial v(x)} ds(y) - \frac{1}{2}\varphi(x) \\ \frac{\partial u}{\partial v}(x) &= \frac{\partial u^i}{\partial v}(x) + \frac{ik}{4}\int_{\Gamma_0} \varphi(y) \frac{\hat{v}(x).\{x-y\} H_1^{(1)}(k|x-y|)}{|x-y|} ds(y) - \frac{1}{2}\varphi(x) \end{aligned} \tag{3.14}$$

The integrals in (3.13) and (3.14) can be accurately evaluated by as fallows,
Total field u on Γ_0 is expressed by using (2.20)

$$u(z_0(t)) = u^i(z_0(t)) + \frac{i}{4}\int_{\Gamma_0} \varphi_\alpha(z_0(t)) H_0^{(1)}(k|z_0(t) - z_0(\tau)|)|z_0'(\tau)| d\tau \tag{3.15}$$

$$u(z_0(t))=u^i(z_0(t))+\sum_{j=0}^{2N-1}\varphi_\alpha(t_j^{(N)})\left\{R_j^{(N)}(t)M_1(t,t_j^{(N)})+\frac{\pi}{N}M_2(t,t_j^{(N)})\right\}\left|z_0'(t_j^{(N)})\right| \quad \textbf{(3.16)}$$

where $t_j^{(N)} = j\pi / N$. Since we only need total field on collocation points, we can find

$$u(z_0(t_m))=u^i(z_0(t_m))+\sum_{j=0}^{2N-1}\varphi_\alpha(t_j^{(N)})\left\{R_{|j-m|}^{(N)}M_1(t_m,t_j^{(N)})+\frac{\pi}{N}M_2(t_m,t_j^{(N)})\right\}\left|z_0'(t_j^{(N)})\right| \quad \textbf{(3.17)}$$

where M_1 and M_2 are given through (2.12-15).

Normal derivative of total field $\partial u / \partial v$ on Γ_0 is given by (3.14) as

$$\frac{\partial u}{\partial v}(x)=\frac{\partial u^i}{\partial v}(x)+(K\varphi)(x)-\frac{\varphi(x)}{2} \quad \textbf{(3.18)}$$

where *K* denote the integral operators defined by

$$(K\varphi)(x)=\int_{\Gamma_0}\frac{\partial\phi(x,y)}{\partial v(x)}\varphi(y)ds(y) \quad \textbf{(3.19)}$$

$$(K\varphi)(z(t))=\frac{-ik}{4}\int_0^{2\pi}\varphi_\alpha(z_0(\tau))\frac{\hat{v}(z_0(t))\{z_0(t)-z_0(\tau)\}}{|z_0(t)-z_0(\tau)|}H_1^{(1)}(k|z_0(t)-z_0(\tau)|)|z_0'(\tau)|d\tau \quad \textbf{(3.20)}$$

Parametrization of (3.20) can be given by

$$(K\varphi)(z_0'(t))=\frac{1}{|x'(t)|}\int_0^{2\pi}H(t,\tau)\varphi_\alpha(z_0(\tau))d\tau \quad \textbf{(3.21)}$$

is given by

$$H(t,\tau)=\frac{ik}{4}v(t).[z_0(\tau)-z_0(t)]\frac{H_1^{(1)}(k|z_0(t)-z_0(\tau)|)}{|z_0(t)-z_0(\tau)|}|z_0'(\tau)| \quad \textbf{(3.22)}$$

where we have set $v(t)=|x'(t)|v(x(t))=(x_2'(t),-x_1'(t))$. We decompose the fundamental solution $H_0^{(1)}=J_0+iN_0$, and use the power series

$$J_0(u)=\sum_{n=0}^{\infty}\frac{(-1)^n}{(n!)^2}\left(\frac{u}{2}\right)^{2n} \quad \textbf{(3.23)}$$

for the Bessel function of order zero and

$$N_0(u)=\frac{2}{\pi}\left(\ln\frac{u}{2}+C\right)J_0(u)+\frac{2}{\pi}\sum_{n=1}^{\infty}\left\{\sum_{m=1}^{n}\frac{1}{m}\right\}\frac{(-1)^{n+1}}{(n!)^2}\left(\frac{u}{2}\right)^{2n} \tag{3.24}$$

for the Neumann function of order zero with Euler constant *C=0.57721…*From these series we can see that the kernel H can be written in the form

$$H(t,\tau)=H_1(t,\tau)\ln\left(4\sin^2\frac{t-\tau}{2}\right)+H_2(t,\tau) \tag{3.25}$$

where

$$H_1(t,\tau)=-\frac{k}{4\pi}v(t).[z_0(\tau)-z_0(t)]\frac{J_1(k|z_0(t)-z_0(\tau)|)}{|z_0(t)-z_0(\tau)|}|z_0'(\tau)| \tag{3.26}$$

$$H_2(t,\tau)=H(t,\tau)-H_1(t,\tau)\ln\left(4\sin^2\frac{t-\tau}{2}\right) \tag{3.27}$$

turn out to be analytic with the diagonal terms

$$H_1(t,t)=0, \tag{3.28}$$

$$H_2(t,t)=\frac{1}{4\pi}\frac{v(t).z_0''(t)}{|z_0'(t)|} \tag{3.29}$$

Using the (2.16) and representation of incident field $u^i(x)=e^{ikx.d}$, normal derivative of the total field can be obtained as

$$\begin{aligned}\frac{\partial u}{\partial v}(z_0(t))=ik(\hat{v}(t).d)e^{ikz_0(t_m).d}-\frac{\varphi_\alpha(t)}{2}+\\ \sum_{j=0}^{2N-1}\varphi_\alpha(t_j^{(N)})\frac{1}{|z_0'(t)|}\left\{R_j^{(N)}(t)H_1(t,t_j^{(N)})+\frac{\pi}{N}H_2(t,t_j^{(N)})\right\}|z_0'(t_j^{(N)})|\end{aligned} \tag{3.30}$$

Since we only need total field on collocation points, we can find

$$\begin{aligned}\frac{\partial u}{\partial v}(z_0(t_m))=ik(\hat{v}(t_m).d)e^{ikz_0(t_m).d}-\frac{\varphi_\alpha(t_m)}{2}+\\ \sum_{j=0}^{2N-1}\varphi_\alpha(t_j^{(N)})\frac{1}{|z_0'(t_m)|}\left\{R_{|j-m|}^{(N)}H_1(t_m,t_j^{(N)})+\frac{\pi}{N}H_2(t_m,t_j^{(N)})\right\}|z_0'(t_j^{(N)})|\end{aligned} \tag{3.31}$$

Since the solution of (3.12) is sensitive to errors in the normal derivative of u in the vicinity of zeros, equation (3.12) is solved in a stable way by a least squares method. For this we express

$$h_0(t) = a_0 + \sum_{j=1}^{J} (a_j \cos jt + a_{J+j} \sin jt) \tag{3.32}$$

as a trigonometric polynomial of degree less than or equal to J. Then, we satisfy (3.12) in a penalized least squares sense, that is, the coefficients $a_0, a_1, ...a_{2J}$ in (3.32) are chosen such that for a set of collocation points $t_0, t_1, ...t_{2N-1}$ in $[0,2\pi)$ the penalized least squares sum

$$\sum_{n=0}^{2N-1} \left| u(z(t_n)) + \frac{\partial u}{\partial v}(z_0(t_n)) h_0(t_n) \right|^2 + \beta_1 \left\{ a_0^2 + \sum_{j=1}^{J} j^{2p} (a_j^2 + a_{j+J}^2) \right\} \tag{3.33}$$

with some regularization parameter $\beta_1 > 0$ and some $p \in N$ is minimized. Here, the penalty term corresponds to the square of the Sobolev norm $\|h_0\|_{H^p}$. We note that the approach can be carried over to other approximations of h_0 rather than by trigonometric polynomials. Substituting (3.17) and (3.31) into (3.33), one obtains,

$$\begin{aligned} &\sum_{n=0}^{2N-1} \left| u^i(z_0(t_n)) + \sum_{j=0}^{2N-1} \varphi_\alpha(t_j^{(N)}) \left\{ R_{|j-n|}^{(N)} M_1(t_n, t_j^{(N)}) + \frac{\pi}{N} M_2(t_n, t_j^{(N)}) \right\} \left| z_0'(t_j^{(N)}) \right| \right. \\ &\left(a_0 + \sum_{h=1}^{J} (a_j \cos(ht_n) + a_{J+h} \sin(ht_n)) \right) \left(ik(\hat{v}(t_n).d) e^{ikz_0(t_n).d} - \frac{\varphi_\alpha(t_n)}{2} + \right. \\ &\left. \left. \sum_{j=0}^{2N-1} \varphi_\alpha(t_j^{(N)}) \frac{1}{|z_0'(t_n)|} \left\{ R_{|j-m|}^{(N)} H_1(t_n, t_j^{(N)}) + \frac{\pi}{N} H_2(t_n, t_j^{(N)}) \right\} \left| z_0'(t_j^{(N)}) \right| \right) \right|^2 \\ &+ \beta_1 \left\{ a_0^2 + \sum_{j=1}^{J} j^{2p} (a_j^2 + a_{j+J}^2) \right\} \end{aligned} \tag{3.34}$$

After the solution of (3.34), new approximation of boundary called as Γ_1 is found through (3.10) and similar procedure is applied for Γ_1 until predetermined stopping condition is satisfied.

3.2 A Second Order Newton Method for Reconstruction of Boundary

A second order method can be performed by modifying (3.12) by using second order derivatives of total field on initial estimation of boundary as [13]

$$u \circ z_0 + \frac{\partial u}{\partial v} \circ z_0 h_0 + \frac{\partial^2 u}{\partial v^2} \circ z_0 h_0^2 = 0 \tag{3.35}$$

The second order derivative $\partial^2 u/\partial v^2$ can be obtained by using the fact that the total field satisfies the Helmholtz equation outside the object, that is, it is given by

$$\frac{\partial^2 u}{\partial v_0^2}\circ z_0 = -k^2 u\circ z_0 + \frac{z_0'.z_0''}{|z_0'|^4}\frac{\partial(u\circ z_0)}{\partial t} - \frac{1}{|z_0'|^2}\frac{\partial^2(u\circ z_0)}{\partial t^2} - \frac{z_0'.v_0'}{|z_0'|^2}\frac{\partial u}{\partial v}\circ z_0 \qquad \textbf{(3.36)}$$

in terms of the parameterization (3.5) [13] (see Appendix A.1). The first and second order derivatives of $u\circ z_0$ with respect to the parameter t occurring in (3.35) can be obtained via trigonometric differentiation. For this purpose, given total field on collocation points $u(t_j),\ \ j=0,1,...2N-1.$ we express the total field by trigonometric interpolation as

$$u(t) = \sum_{j=0}^{2N-1} u(t_j)L(t,t_j) \qquad \textbf{(3.37)}$$

where

$$L(t,t_j) = \frac{1}{2N}\sin(N(t-t_j))\cot\left(\frac{t-t_j}{2}\right) \qquad \textbf{(3.38)}$$

is Lagrange basis or interpolating polynomial. Derivative with respect to parameter t can be given as

$$u'(t) = \sum_{j=0}^{2N-1} u(t_j)L'(t,t_j) \qquad \textbf{(3.39)}$$

where $L'(t,t_j)$ is derivative of $L(t,t_j)$ given by

$$L'(t,t_j) = \frac{1}{2N}\left(N\cos(N(t-t_j))\cot\left(\frac{t-t_j}{2}\right) - \frac{1}{2}\frac{\sin(N(t-t_j))}{\sin^2((t-t_j)/2)}\right) \qquad \textbf{(3.40)}$$

since we need derivative only collocation points and obtaining $L'(t,t_j)$ as $t\to t_j$ by

$$\lim_{t\to t_j}\frac{1}{2N}\left(N\cos(N(t-t_j))\cot\left(\frac{t-t_j}{2}\right) - \frac{1}{2}\frac{\sin(N(t-t_j))}{\sin^2((t-t_j)/2)}\right) = 0 \qquad \textbf{(3.41)}$$

one obtains

$$u'(t_m) = \sum_{j=0,m\neq j}^{2N-1} u(t_j)\frac{1}{2N}\left(N\cos(N(t_m-t_j))\cot\left(\frac{t_m-t_j}{2}\right) - \frac{1}{2}\frac{\sin(N(t_m-t_j))}{\sin^2((t_m-t_j)/2)}\right) \qquad \textbf{(3.42)}$$

As seen from (3.35), one also needs second order derivative with respect to t in order to calculate second order normal derivative, second order derivative with respect to t can be calculated by similar way as

$$u''(t) = \sum_{j=0}^{2N-1} u'(t_j) L'(t, t_j) \tag{3.43}$$

$$u''(t_p) = \sum_{m=0,\, p\neq m}^{2N-1} \sum_{j=0, m\neq j}^{2N-1} u(t_j) \frac{1}{2N} \left(N \cos(N(t_m - t_j)) \cot\left(\frac{t_m - t_j}{2}\right) - \frac{1}{2} \frac{\sin(N(t_m - t_j))}{\sin^2((t_m - t_j)/2)} \right) \frac{1}{2N} \left(N \cos(N(t_p - t_m)) \cot\left(\frac{t_p - t_m}{2}\right) - \frac{1}{2} \frac{\sin(N(t_p - t_m))}{\sin^2((t_p - t_m)/2)} \right) \tag{3.44}$$

As in the work of Hettlich and Rundell [19] and following Halley [27] the nonlinear equation (3.35) is solved in two steps, a predictor and a corrector step. In the predictor step, one has to solve

$$u \circ z_0 + \frac{\partial u}{\partial v} \circ z_0 h_{0,1} = 0 \tag{3.45}$$

for $h_{0,1}$ which is solved by procedure in Section (3.1).

Once h_0 has been obtained, in the corrector step the equations [13]

$$u \circ z_0 + \frac{\partial u}{\partial v} \circ z_0 h_{0,2} + \frac{\partial^2 u}{\partial v^2} \circ z_0 h_{0,1} h_{0,2} = 0 \tag{3.46}$$

are solved for $h_{0,2}$ again in a penalized least squares sense, that is, the coefficients in

$$h_{0,2}(t) = b_0 + \sum_{j=1}^{J} \left\{ b_j \cos jt + b_{J+j} \sin jt \right\} \tag{3.47}$$

are chosen such that [13]

$$\sum_{n=0}^{2N-1} \left| u(z_0(t_n)) + \left[\frac{\partial u}{\partial v}(z_0(t_n)) + \frac{1}{2} \frac{\partial^2 u}{\partial v^2}(z_0(t_n)) h_{0,1}(t_n) \right] h_{0,2}(t_n) \right|^2 + \beta_2 \left\{ b_0^2 + \sum_{j=1}^{J} j^{2p} \left(b_j^2 + b_{J+j}^2 \right) \right\} \tag{3.48}$$

with some regularization parameter $\beta_2 > 0$ is minimized. Then, finally $h = h_{0,2}$ is inserted in (3.10) to obtain the updated boundary Γ_1. This procedure of alternatingly

solving (3.2) and (3.35) now is iterated in an obvious fashion until some stopping criterium is satisfied.

Although there are a few results available on the convergence of regularized Newton iterations for inverse obstacle scattering problems (see [19, 28, 29, 30]) this issue is not satisfactorily resolved. Despite the progress made by Hohage [28, 29] with this espect, so far it has not been clarified whether the general results on the solution of ill-posed nonlinear equations in a Hilbert space setting (among others see [31, 32]) are applicable to inverse obstacle scattering or, in general, to inverse boundary value problems in the frame work of solving the operator equation (1.7). This remark also implies to the convergence results of Hettlich and Rundell [19] on the second order method with respect to its applicability for the inverse obstacle scattering problem.

The more problem oriented approach of Potthast [30] for a convergence analysis suffers from the restrictive assumption of a non vanishing normal derivative of the total field on the boundary ∂D in the case of exact data. Furthermore, in the analysis for noisy data, convergence for the noise level tending to zero, as usual, requires a stopping rule and with this particular rule the method has not yet been numerically implemented.

These comments also apply to the case of the first order method of Kress and Serranho. At present only convergence results in the spirit of Potthast [30] are available in [17]. Therefore, we view it as legitimate to present our second order variant of this approach without a detailed convergence analysis and confine ourselves to some heuristic considerations.

We begin with the case of exact far field data u_∞. Since we assume ∂D to be analytic, the solution to the scattering problem has an extension as a solution to the Helmholtz equation across ∂D in some neighborhood. If Γ_0 is contained in this neighborhood and provided k^2 is not a Dirichlet eigenvalue for the negative Laplacian in the interior of Γ_0 then the far field equation (3.2) is uniquely solvable and its solution represents the scattered field via (3.1). Consequently our second order method as formulated in (3.16) corresponds to a second order Newton method for finding the zero level curve of the exact total field u. Under the assumption that the normal derivative of u does not vanish on Γ_0 (this can be shown to be valid in the case of scattering from a disk) then as in [17, 30] and using the convergence result of Hettlich and Rundell [19] for the second order Newton method for an

operator with a bijective and bounded Frechet derivative in can be verified that our second order method has convergence order three.

Of course, as in all of the iterative methods for the inverse obstacle scattering problem, the ill-posedness corrupts the high order convergence. Here, the ill-posedness enters through the integral equation (3.2) of the first kind leading to inevitable errors occurring in its regularized solution. It is to be expected that a convergence analysis with respect to the noise level can be carried out analogous to the first order method as described in [17]. We refrain from working out the details since the result would be of a qualitative character only and would not lead to the possibility for a quantitative comparison on the convergence for the first and second order method. However, from the better convergence order for the exact data case one might expect some advantages in the numerical performance. Indeed, our numerical examples in the next section illustrate an improvement in the quality of the reconstructions and the speed of convergence connected with an increase in the stability with respect to noisy data.

3.3 Extension of Newton Reconstruction Method for Multi-view illumination

Proposed first and second order Newton reconstruction methods in section 3.1 and 3.2 can be extended straightforwardly for multi illumination cases. In this case, object is illuminated by multi plane waves separately each having different propagation direction. Scattered data is obtained on unit circle Ω for each illumination. In this case, one obtains single layer density for each illumination as fallows,

$$(S_\infty \varphi^{(n)})(\hat{x}) = u_\infty^{(n)}(\hat{x}), \quad n = 1,2,...L \tag{3.49}$$

where $\varphi^{(n)}$ and $u_\infty^{(n)}$ represent single layer density and far field pattern for n. illumination respectively. L is total number of the illuminations. Single layer density on initial estimate of the boundary related for each illumination can be obtained as,

$$\varphi^{(n)}(x) = (\alpha I + S_\infty^* S_\infty)^{-1} S_\infty^* u_\infty^{(n)}, \ x \in \Gamma_0, \quad n = 1,2,...L \tag{3.50}$$

Total field and its normal derivative on the initial estimate of the boundary can be expressed as,

$$u^{(n)}(x) = u_s^{(n)}(x) + u_i^{(n)}(x), \quad x \in \Gamma_0, \quad n = 1,2,....L \tag{3.51}$$

where $u_s^{(n)}(x)$ is scattered field related with n. illumination given by

$$u_s^{(n)}(x) = \int_{\Gamma_0} \varphi^{(n)}(y)\phi(x,y)ds(y), \quad x \in \Gamma_0, \quad n = 1,2...L \tag{3.52}$$

and $u_i^{(n)}(x) = e^{ikx.d_n}$ n. illumination with propagation direction d_n .Normal derivative of the total field on the initial estimate of the boundary related with n. illumination can expressed as,

$$\frac{\partial u^{(n)}(x)}{\partial v} = \frac{\partial u_s^{(n)}(x)}{\partial v} + \frac{\partial u_i^{(n)}(x)}{\partial v}, \quad x \in \Gamma_0, \quad n = 1,2,....L \tag{3.53}$$

Substituting (3.52) on (3.53) and using the representation n. illumination of incident field, (3.53) can be written as,

$$\frac{\partial u^{(n)}(x)}{\partial v} = \int_{\Gamma_0} \varphi^{(n)}(y)\frac{\partial \phi(x,y)}{\partial v(x)}ds(y) + ik\hat{v}(x).d_n e^{ikx.d_n}, \quad x \in \Gamma_0, \quad n = 1,2,....L \tag{3.54}$$

and one obtains the equation set given for first order Newton method as

$$u^{(n)}(x) + h(x)\frac{\partial u^{(n)}}{\partial v}(x)\bigg|_{\Gamma_0} = 0, \quad x \in \Gamma_0, \quad n = 1,2,...L \tag{3.55}$$

and for second order Newton method as

$$u^{(n)}(x) + h(x)\frac{\partial u^{(n)}}{\partial v}(x)\bigg|_{\Gamma_0} + h^2(x)\frac{\partial^2 u^{(n)}}{\partial v^2}(x)\bigg|_{\Gamma_0} = 0, \quad x \in \Gamma_0, \quad n = 1,2,...L \tag{3.56}$$

that can be solved solved straightforwardly by methods described in section 3.1 and section 3.2 respectively.

3.5 Extension of Newton Reconstruction Methods for PEC Objects Located on Known Domain

Proposed Newton reconstruction methods can be extended for reconstruction of perfectly electric conducting (PEC) objects located on known domain by using the fundamental solution of Helmholtz equation on known domain and its far field pattern and using the incident field as field in the absence of the PEC object. Fundamental solution of Helmoltz equation on known domain $\phi(x,y)$ simply is total field on x if line source located on y . This is well known direct scattering problem.

Therefore, $\phi(x, y)$ can be obtained straightforwardly. Field in the absence of the PEC object can also be obtained via direct scattering problem for plane wave excitation. Using these interchanging on section 3.1 and section 3.2, it is possible proposed Newton methods for reconstruction of PEC objects located in known domain.

4. A SECOND ORDER NEWTON METHOD FOR SHAPE RECONSTRUCTION OF BURIED OBJECTS

In this section, A second order Newton method for reconstructing the shape of a perfectly electrical conducting (PEC) scatterer buried in an arbitrary shaped dielectric cylinder from the measured far-field pattern is presented. Object as depicted in fig.4.1 is illuminated by incident field $u^i = e^{ik_1 x.\hat{k}_i}$ that is polarized along x_3 axis with propagation direction $\hat{k}_i = -(\cos(\phi_0)\hat{x}_1 + \sin(\phi_0)\hat{x}_2)$. Because of the homogeneity of the problem with respect to x_3 axis, scattered field is also x_3 polarized and problem reduces scalar problem in $x \in R^2$. Let's call the total field in the absence of the PEC object as u^0 then straightforward direct scattering problem consists of finding the total field $u = u^0 + u^s$ as the sum of the known field u^0 and scattered field u^s that is result of PEC object with boundary ∂D buried inside the dielectric medium with boundary ∂C and wave number k_2 as depicted fig.4.1. Let's represent the total field $u(x)$, as $u(x) = u_2(x), x \in C$ and $u(x) = u_1(x), x \in R^2 \setminus \mathrm{C}$ such that total field satisfies the Helmholtz equation

$$\begin{aligned} &\Delta u_1(x) + k_1^2 u_1(x) = 0, \quad x \in R^2 \setminus \mathrm{C} \\ &\Delta u_2(x) + k_2^2 u_2(x) = 0, \quad x \in C \end{aligned} \tag{4.1}$$

with k_1 and k_2 that are wave number of background medium and dielectric cylinder respectively, also satisfies the PEC boundary condition

$$u(x) = 0, \quad x \in \partial D \tag{4.2}$$

and boundary condition on dielectric interface ∂C as

$$\begin{aligned} &u_2(x) = u_1(x), \quad x \in \partial C \\ &\frac{\partial u_2}{\partial v}(x) = \frac{\partial u_1}{\partial v}(x), \quad x \in \partial C \end{aligned} \tag{4.3}$$

where $\partial / \partial v$ is normal derivative, and the scattered wave u^s satisfies the Sommerfeld radiation condition as

$$\lim_{r\to\infty} \sqrt{r}\left(\frac{\partial u^s}{\partial r} - ik_1 u^s \right) = 0, \qquad r = |x| \tag{4.4}$$

uniformly with respect to all directions on unit circle Ω and the scattered wave has a asymptotic behavior as

[1]

$$u^s(x) = \frac{e^{ik_1|x|}}{\sqrt{|x|}} \left\{ u_\infty(\hat{x}) + O\left(\frac{1}{|x|} \right) \right\}, \quad |x| \to \infty, \qquad \hat{x} \in \Omega \tag{4.5}$$

with $\hat{x} = x/|x| = (\cos\phi, \sin\phi), \phi \in [0, 2\pi)$, uniformly in all directions with the far field pattern u_∞ defined on the unit circle Ω.

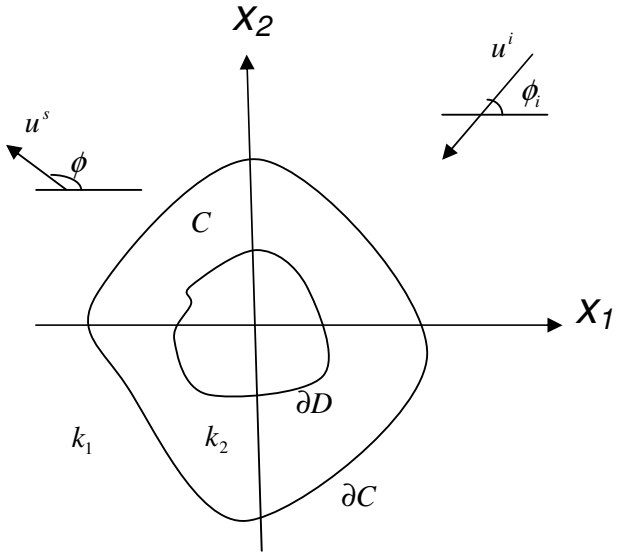

Figure 4.1: Geometry of the considered problem.

The inverse obstacle problem is the determination of boundary ∂D by means of the given far field pattern $u_\infty(\hat{x}), \hat{x} \in \Omega$ with the knowledge of the wave numbers k_1, k_2 and boundary of the dielectric cylinder ∂C and incident field u^i. The direct

scattering problem can be represented by an operator as $F:\partial D \to u_\infty$ that maps the boundary ∂D onto the far field pattern u_∞. By using this operator, given a far field pattern u_∞, the inverse problem is expressed as the solution of nonlinear and ill-posed operator equation,

$$F(\partial D) = u_\infty \tag{4.6}$$

for the unknown surface ∂D. Because of the facts that direct scattering problem depends nonlinearly on the boundary, Eq. (4.6) is nonlinear. Also, it is ill posed since the far field pattern is an analytic function on the unit circle Ω.

The presented Newton iteration starts with an initial estimate Γ_0 of the boundary ∂D. The scattered field in the closed exterior of Γ_0 can be expressed by using single layer potential [4]

$$(P_{\Gamma_0}\varphi)(x) = \int_{\Gamma_0} G(x,y)\varphi(y)ds(y), \quad x \in R^2 / \Gamma_0 \tag{4.7}$$

with density $\varphi \in L^2(\Gamma_0)$ in the exterior of the surface Γ_0, where

$$G(x,y) = \begin{cases} G_t(x,y), & x \in R^2 \setminus \mathrm{C},\ y \in C \\ \dfrac{i}{4}H_0^{(1)}(k_2|x-y|) + G_r(x,y), & x \in C,\ y \in C \end{cases} \tag{4.8}$$

represents the Green's function of Helmoltz equation in the domain containing dielectric cylinder (see Appendix A.2). Where $H_0^{(1)}(.)$ denotes the zero order Hankel function of the first kind. In (3.64), the terms $G_t(x,y)$ and $G_r(x,y)$ are smooth part of Green's function given in Appendix A.2 [23]

The far field pattern of the potential (4.7) for the scattered direction $\hat{x} = (\cos\phi, \sin\phi), \phi \in (0, 2\pi)$ as shown in Fig.1, denoted by $(P_{\Gamma_0,\infty}\varphi)(\hat{x})$ can be derived from $G_t(x,y)$ while $|x| \to \infty$ as (see Appendix A.2) [23]

$$(P_{\Gamma_0,\infty}\varphi)(\hat{x}) = \frac{e^{i\pi/4}}{\sqrt{8\pi k_1}} \int_{\partial C} e^{-ik_1 \hat{x}.g} \int_{\Gamma_0} \Phi(g,y)\varphi(y)ds(y)ds(g) \tag{4.9}$$

Because of the fact that the scattered field u^s is uniquely determined by its far field pattern u_∞, the density φ can be seen to be the unique solution of the ill posed integral equation

$$\frac{e^{i\pi/4}}{\sqrt{8\pi k_1}} \int_{\partial C} e^{-ik_1 \hat{x}.g} \int_{\Gamma_0} \Phi(g,y)\varphi(y)ds(y)ds(g) = u_\infty(\hat{x}) \qquad \textbf{(4.10)}$$

Due to its analytic kernel, integral equation in (4.10) is severely ill posed [23]. However, the operator $P_{\Gamma_0,\infty} : L^2(\Gamma_0) \to L^2(\Omega)$ in (4.9) is known to be injective and has dense range. Therefore, Tikhonov regularization can be applied for a stable approximate solution of (10), that is, the ill-posed equation (4.10) is replaced by

$$\alpha\varphi + P^*_{\Gamma_0,\infty} P_{\Gamma_0,\infty}\varphi = P^*_{\Gamma_0,\infty} u_\infty \qquad \textbf{(4.11)}$$

with some positive regularization parameter α and the adjoint $P^*_{\Gamma_0,\infty}$ of $P_{\Gamma_0,\infty}$.

For the further description of the reconstruction scheme we represent the curve Γ_0 by a regular parameterization

$$\Gamma_0 = \{z_0(t) : t \in [0,2\pi)\} \qquad \textbf{(4.12)}$$

with a 2π periodic function $z_0 : R \to R^2$. Searching the location where the boundary condition (4.12) is satisfied, we approximate the total field u by the Taylor formula of order two with respect to the normal direction at Γ_0. For this purpose, we try to update in the form

$$\Gamma_1 = \{z_1(t) = z_0(t) + h(t)v_0(t) : t \in [0,2\pi)\} \qquad \textbf{(4.13)}$$

where v_0 denotes the outward normal vector to Γ_0 and $h : IR \to IR$ is a sufficiently small 2π periodic function. The normal vector can be expressed through the parameterization (4.12) via

$$v_0(t) = \frac{(z_0'(t))^\perp}{|z_0'(t)|}, \quad t \in [0,2\pi) \qquad \textbf{(4.14)}$$

where for any vector $a = (a_1, a_2)$, we set $a^\perp = (a_2, -a_1)$. Then the first order Taylor formula requires the update function h to satisfy

$$u + \left.\frac{\partial u}{\partial v_0}\right|_{\Gamma_0} h + \frac{1}{2}\left.\frac{\partial^2 u}{\partial v_0^2}\right|_{\Gamma_0} h^2 = 0 \qquad \textbf{(4.15)}$$

Once the single layer density φ is known from (4.11), the values u and normal derivative $\partial u / \partial v_0$ of the total field on Γ_0 can be obtained through the jump relations for the single-layer potential [4], that is, by

$$u(x) = u^0(x) + \int_{\Gamma_0} \phi(x, y)\varphi(y)ds(y), \qquad x \in \Gamma_0 \tag{4.16}$$

$$\frac{\partial u}{\partial v}(x) = \frac{\partial u^0}{\partial v}(x) + \int_{\Gamma_0} \frac{\partial \phi(x, y)}{\partial v(x)}\varphi(y)ds(y) - \frac{1}{2}\varphi(x), \qquad x \in \Gamma_0 \tag{4.17}$$

where $u^0(x)$ is the total field in the absence of the PEC object (see Appendix A.3). The second order derivative $\partial^2 u / \partial v_0^2$ can be obtained by using the fact that the total field satisfies the Helmholtz equation outside the object, that is, it is given by

$$\frac{\partial^2 u}{\partial v_0^2} = -k_2^2 u + \frac{z_0'.z_0''}{|z_0'|^4}\frac{\partial u}{\partial t} - \frac{1}{|z_0'|^2}\frac{\partial^2 u}{\partial t^2} - \frac{z_0'.v_0'}{|z_0'|^2}\frac{\partial u}{\partial v_0} \tag{4.18}$$

in terms of the parameterization given in (4.12) [13]. The integrals in (4.16) and (4.17) can be accurately evaluated by the quadrature rules as described in [4] and the first and second order derivatives of u with respect to the parameter t occurring in (4.18) can be obtained via trigonometric differentiation.

As in the work of Hettlich and Rundell [19] and following Halley [27] the nonlinear equation (4.15) is solved in two steps, a predictor and a corrector step. In the predictor step, one has to solve

$$u + \left.\frac{\partial u}{\partial v_0}\right|_{\Gamma_0} h_0 = 0 \tag{4.19}$$

for h_0. Since the solution of (4.19) is sensitive to errors in the normal derivative of u in the vicinity of zeros, equation (4.19) is solved in a stable way by a least squares method. For this we express

$$h_0(t) = a_0 + \sum_{j=1}^{J} (a_j \cos(jt) + a_{J+j} \sin(jt)) \tag{4.20}$$

as a trigonometric polynomial of degree less than or equal to J. Then, we satisfy (4.19) in a penalized least squares sense, that is, the coefficients $a_0, a_1, \ldots a_{2J}$ in

(4.20) are chosen such that for a set of collocation points $t_1, t_2, ...t_N$ in $[0,2\pi)$ the penalized least squares sum

$$\sum_{n=1}^{N}\left|u(z_0(t_n))+\frac{\partial u}{\partial v_0}(z_0(t_n))h_0(t_n)\right|^2+\beta_1\left\{a_0^2+\sum_{j=1}^{J}j^{2p}(a_j^2+a_{j+J}^2)\right\} \quad \textbf{(4.21)}$$

with some regularization parameter $\beta_1 > 0$ and some $p \in N$ is minimized. Here, the penalty term corresponds to the square of the Sobolev norm $\|h_0\|_{H^p}$

Once h_0 has been obtained, in the corrector step the equation

$$u+\frac{\partial u}{\partial v_0}\bigg|_{\Gamma_0}h+\frac{1}{2}\frac{\partial^2 u}{\partial v_0^2}\bigg|_{\Gamma_0}h.h_0=0 \quad \textbf{(4.22)}$$

is solved again in a penalized least squares sense, that is, the coefficients in

$$h(t)=b_0+\sum_{j=1}^{J}(b_j\cos(jt)+b_{J+j}\sin(jt)) \quad \textbf{(4.23)}$$

are chosen such that [13]

$$\sum_{n=1}^{N}\left|u(z_0(t_n))+\left[\frac{\partial u}{\partial v_0}(z_0(t_n))+\frac{1}{2}\frac{\partial^2 u}{\partial v_0^2}(z_0(t_n))h_0(t_n)\right]h(t)\right|^2+\beta_2\left\{b_0^2+\sum_{j=1}^{J}j^{2p}(b_j^2+b_{j+J}^2)\right\} \quad \textbf{(4.24)}$$

with some regularization parameter $\beta_2 > 0$ is minimized. Then, finally $h(t)$ is inserted in (4.23) to obtain the updated boundary Γ_1. This procedure of alternatingly solving (4.11) and (4.15) now is iterated in an obvious fashion until some stopping criterium is satisfied.

We demonstrated the proposed second order Newton method for reconstruction of PEC scatterers buried inside the dielectric cylinder of arbitrary shape by some examples. In all our examples we used N = 50 equidistant collocation points in the least squares sums in (4.21) and (4.24). Accordingly, we used 50 equidisant collocation points on $[0,2\pi)$ in the parametric representation of Γ_0 and 50 equidisant data points for the far field pattern on the unit circle Ω. The latter, in particular, means that we require full aperture data. In order to avoid an inverse crime, the synthetic data were obtained by solving the combined single- and double-layer boundary integral equation for the direct scattering problem by the Nyström method as described in [4] with 100 quadrature points. The wave number of exterior medium

is chosen as $k_1 = 1$ and the penalty factors for the least squares approach as $\beta_1 = \beta_2 = 0.0001$. Tikhonov regularization parameter α is chosed as 10^{-8} for exact data and 10^{-4} for noisy data. The Sobolev norm parameter and polynomial degree were chosen as *p = 3* and *J=6* respectively. All iterations were started with circle of radius 1m. To introduce a stopping criterium, we consider the residual

$$res_n = \left\| u(x) \right\|_{L^2}, \quad x \in \Gamma_n \tag{4.25}$$

that is L^2 norm of total field on boundary Γ_n obtained at n. iteration. In our examples we terminated the iterations when one of the two conditions is satisfied.

$$\left| res_{n+1} - res_n \right| \le 0.01 \quad \text{or} \quad res_n \le 0.01 \tag{4.26}$$

In order to demonstrate that second order Newton method is more effective than first order method, change of residuals obtained by first and second order Newton methods are given in Tables.

In the first example, we consider the reconstruction of the peanut shaped PEC object located inside a elliptical cylinder whose wave number and radius are $k_2 = 2 + 0.1i$, $a = 2$ respectively. Angle of incidence is chosen as $\phi_0 = \pi / 2$ therefore $d = (0,-1)$. The parameterization of the boundaries of dielectric and PEC objects given respectively as

$$\partial C = \left\{ (2\cos t, 1.5\sin t),\ t \in [0, 2\pi) \right\} [m] \tag{4.27}$$

$$\partial D = \left\{ (\sqrt{\cos^2 t + 0.25\sin^2 t})(\cos t, \sin t),\ t \in [0, 2\pi) \right\} [m] \tag{4.28}$$

Far field pattern of buried peanut shaped object for $d = (0,-1)$ incident direction is depicted in fig.4.2. The reconstructions of buried peanut shaped object for $d = (0, -1)$ incident direction and using exact and %3 noisy data are given by figure 4.3 and figure 4.4 respectively. The change of the residual given in (4.25) during the iterations is illustrated through Table 4.15 for exact data.

In the second example, we consider the reconstruction of the kite shaped PEC object located inside cylinder whose wave number $k_2 = 1.6 + 0.07i$ and parametrization given in (4.29). Angle of incidence is chosen as $\phi_0 = 0$ therefore $d = (-1,0)$. The

parameterization of the boundaries of dielectric cylinder and kite shaped PEC objects given respectively as

$$\partial C = \{(3 + 0.6\sin(3t))(\cos t, \sin t),\ t \in [0, 2\pi)\}\ [m] \tag{4.29}$$

$$\partial D = \{(\cos t + 0.65\cos 2t - 0.15,\ 1.5\sin t),\ t \in [0, 2\pi)\}\ [m] \tag{4.30}$$

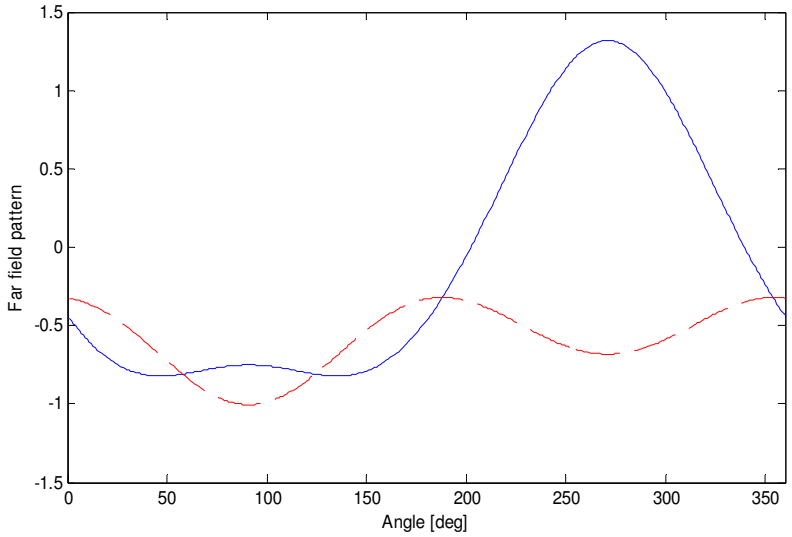

Figure 4.2 : Far field pattern of the buried peanut shaped object for $d = (0, -1)$.

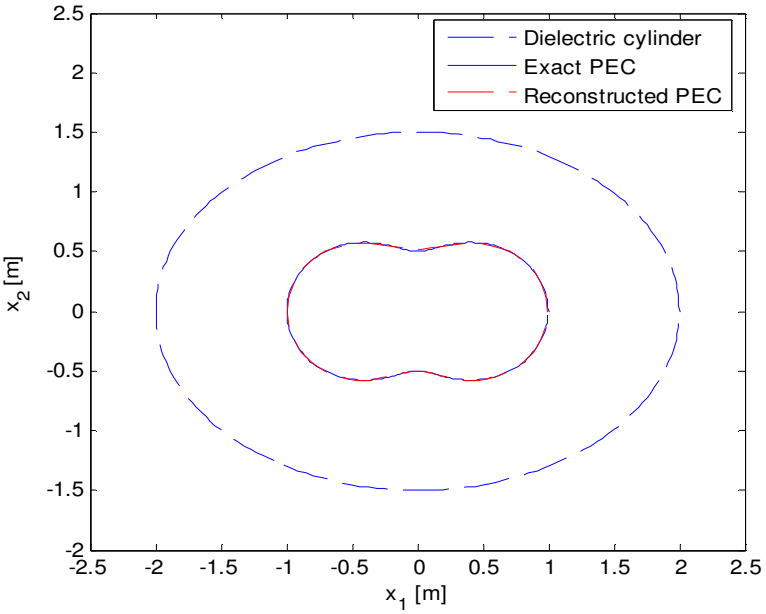

Figure 4.3 : Reconstruction of buried peanut object for $d = (0, -1)$ and exact data.

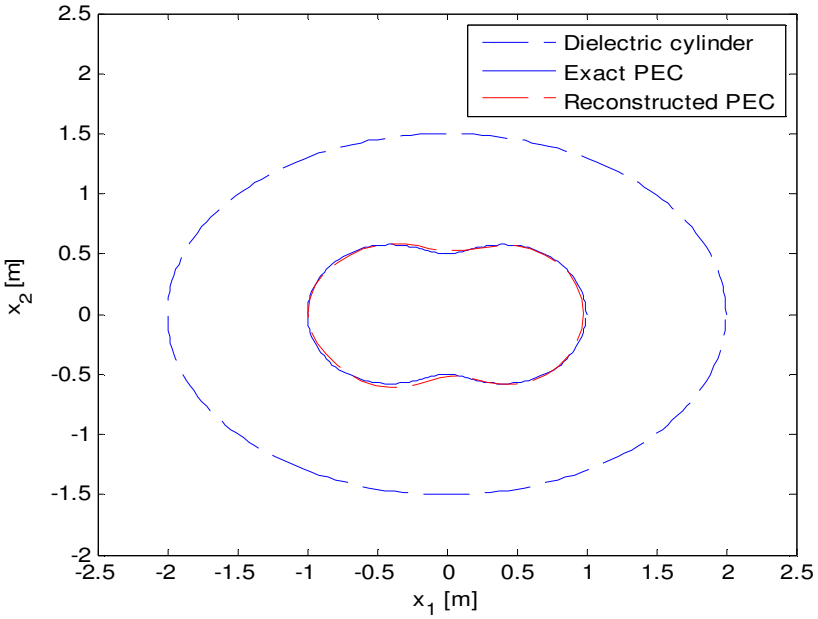

Figure 4.4: Reconstruction of buried peanut shaped object for $d = (0,-1)$ and %3 noisy data.

Far field pattern of buried kite shaped object for $d = (-1,0)$ incident direction is depicted in fig.4.5. The reconstructions of buried peanut shaped object for $d = (0,-1)$ incident direction and using exact and %3 noisy data are given by figure 4.6 and figure 4.7 respectively. The change of the residual expressed in (4.25) during the iterations is illustrated through Table 4.1 for exact data.

Table 4.1: Residuals of buried peanut shaped object for $d = (0,-1)$ and exact data.

Iteration number	First order Newton	Second order Newton
0 (initial estimate)	4.056	4.056
1	0.936	0.754
2	0.241	0.115
3	0.199	0.0065
4	0.186	--
5	0.184	--

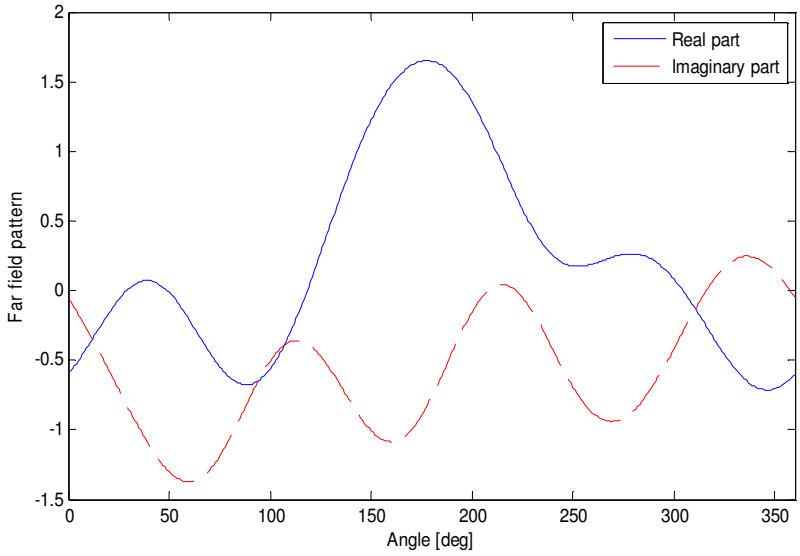

Figure 4.5 : Far field pattern of the buried kite shaped object for $d = (-1,0)$.

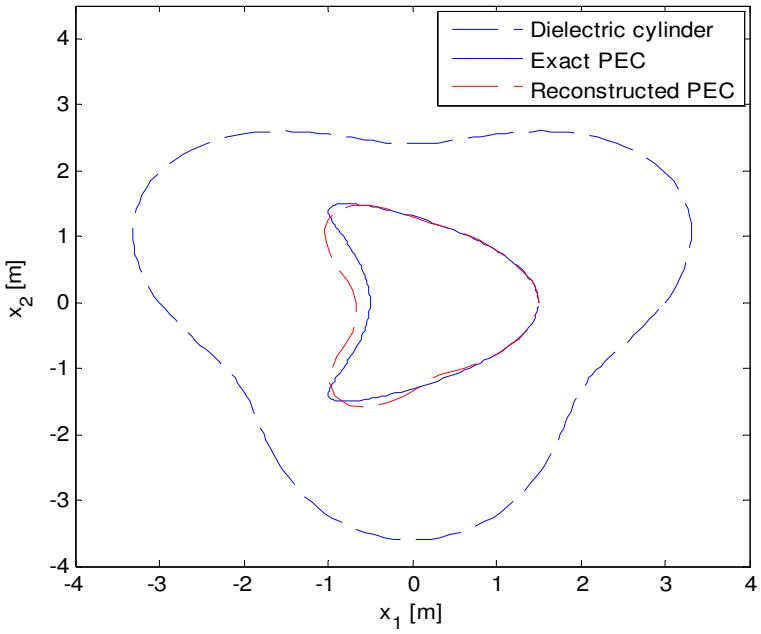

Figure 4.6 : Reconstruction of buried kite object for $d = (-1,0)$ and exact data.

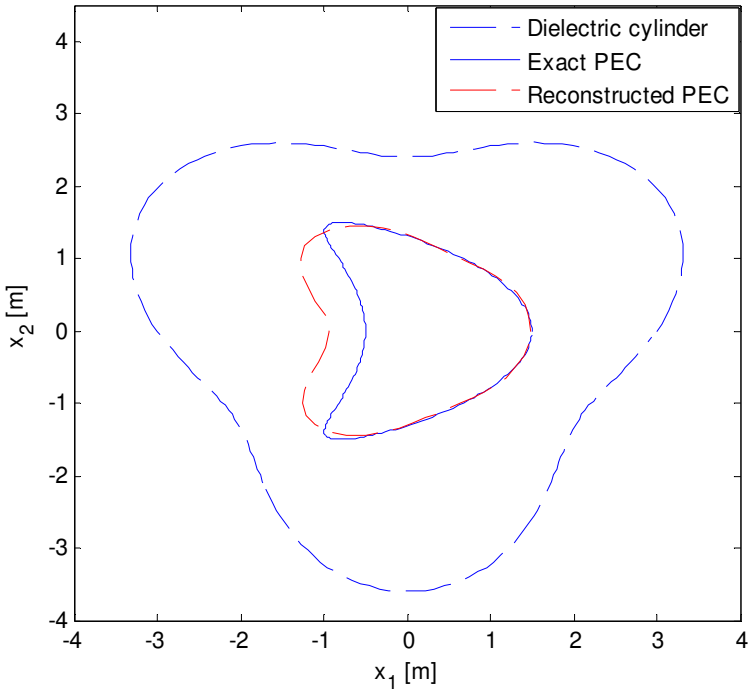

Figure 4.7 : Reconstruction of buried kite object for $d = (-1,0)$ and %3 noisy data.

Table 4.2 : Residuals of buried kite shaped object for $d = (-1, 0)$ and exact data.

Iteration number	First order Newton	Second order Newton
0 (initial estimate)	6.948	6.948
1	2.562	1.146
2	0.868	0.541
3	0.464	0.276
4	0.412	0.267
5	0.391	--
6	0.378	--
7	0.371	

5. NUMERICAL EXAMPLES

In all our examples, we used N = 50 equidistant collocation points in the least squares sums in (3.33) and (3.48). Accordingly, we used 50 equidisant collocation points on $[0,2\pi)$ in the parametric representation of and 50 equidisant data points for the far field pattern on the unit circle . The latter, in particular, means that we require full aperture data. In order to avoid an inverse crime, the synthetic data were obtained by solving the combined single- and double-layer boundary integral equation for the direct scattering problem by the Nyström method as described in section 2.1 with 100 quadrature points. The wave number is chosen as $k = 1$ and the penalty factors for the least squares approach as $\beta_1 = \beta_2 = 0.00001$. The Sobolev norm parameter was chosen as $p = 3$.

For selecting the Tikhonov regularization parameter α in (3.4), we employed the discrepancy principle as described, for example, in [9], that is, α is chosen such that

$$\left\| S_\infty (\alpha I + S_\infty^* S_\infty)^{-1} S_\infty^* u_\infty - u_\infty \right\|_{L^2} = \delta \qquad \textbf{(5.1)}$$

where $\delta = 10^{-7}$ for exact data and $\delta = 10^{-4}$ for noisy data. To introduce a stopping criterium we consider the residual

$$res_{n,J} = \left\| A(\Gamma_{n,J}) - u_\infty \right\|_{L^2} \qquad \textbf{(5.2)}$$

between the given far field data u_∞ and the far field pattern $A(\Gamma_{n,J})$ for the approximate boundary $\Gamma_{n,J}$ obtained after n iteration steps using the trigonometric polynomial degree J. In our examples we terminated the iterations when

$$res_{n,J} \le 10^{-2} \left\| u_\infty \right\|_{L^2} \quad \text{or} \quad \left| res_{n,J} - res_{n-1,J} \right| \le 10^{-2} \qquad \textbf{(5.3)}$$

for exact data and

$$res_{n,J} \le 2.10^{-2}\left\|u_{\infty}\right\|_{L^2} \quad \text{or} \qquad \left|res_{n,J} - res_{n-1,J}\right| \le 2.10^{-2} \tag{5.4}$$

for noisy data. We observed different final residuals for different trigonometric polynomial degree J and for the figures we chose J such that this residual is minimal. For comparison, we executed both the first and second order Newton method.

It is also observed that each iteration step requires 1.7083s and 1.7147s for the first and second order Newton methods respectively, if computer with 1800MHz clock frequency is used.

In the first example, we consider the identification of a peanut-shaped object with the parameterization,

$$\partial D = \left\{\sqrt{\cos^2 t + 0.25\sin^2 t}\ (\cos t, \sin t) : t \in [0, 2\pi)\right\}[m] \tag{5.5}$$

for two different angles of incidence. Poynomial degree $J = 6$ was selected.
For the incident directions $d = (-1,0)$ and $d = (-1/\sqrt{2}, -1/\sqrt{2})$, Iteration was started with a circle of radius 1.5m and 0.5m respectively. For exact data, the change of the residual during the iterations for the incident directions $d = (-1,0)$ and $d = (-1/\sqrt{2}, -1/\sqrt{2})$ are illustrated through Table 5.1 and Table 5.2 respectively and for noisy data, illustrated through Table 5.3 and Table 5.4 respectively.

Table 5.1 : Residuals of Peanut object for $d = (-1,0)$ and exact data.

Iteration number	First order Newton	Second order Newton
0 (initial estimate)	5.9390	5.9390
1	1.5877	0.8427
2	0.3325	0.0074
3	0.0391	--

Table 5.2 : Residuals of Peanut object for $d = (-1/\sqrt{2}, -1/\sqrt{2})$ and exact data.

Iteration number	First order Newton	Second order Newton
0 (initial estimate)	2.9496	2.9496
1	1.5253	0.3193
2	0.4849	0.0122
3	0.0391	--

Table 5.3 : Residuals of Peanut object for $d = (-1,0)$ and %3 noisy data.

Iteration number	First order Newton	Second order Newton
0 (initial estimate)	5.8476	5.8476
1	1.5244	0.8160
2	0.3096	0.0999
3	0.1357	--
4	0.1352	--

Table 5.4 : Residuals of Peanut object for $d = (-1/\sqrt{2},-1/\sqrt{2})$ and %3 noisy data.

Iteration number	First order Newton	Second order Newton
0 (initial estimate)	3.0692	3.0692
1	1.1165	0.4633
2	0.3167	0.1318
3	0.2035	--
4	0.1831	--
	0.1813	--

Far field patterns of peanut shaped object for $d = (-1,0)$ and $d = (-1/\sqrt{2},-1/\sqrt{2})$ incident directions are depicted in fig.5.1 and fig.5.2 respectively. The reconstructions of peanut shaped object for $d = (-1,0)$ incident direction and exact and %3 noisy data are given by figure 5.3 and figure 5.4 respectively.The reconstructions of peanut shaped object for $d = (-1/\sqrt{2},-1/\sqrt{2})$ incident direction exact and %3 noisy data are given by figure 5.5 and figure 5.6 respectively.

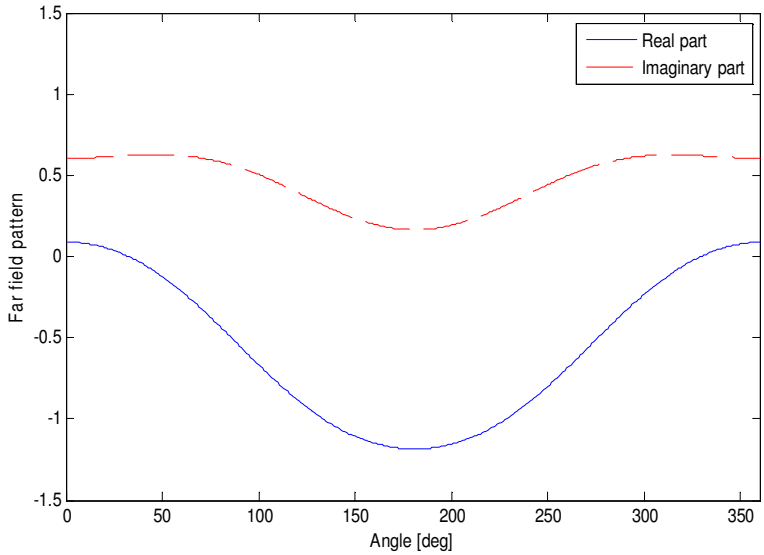

Figure 5.1 : Far field pattern of peanut shaped object for $d = (-1,0)$.

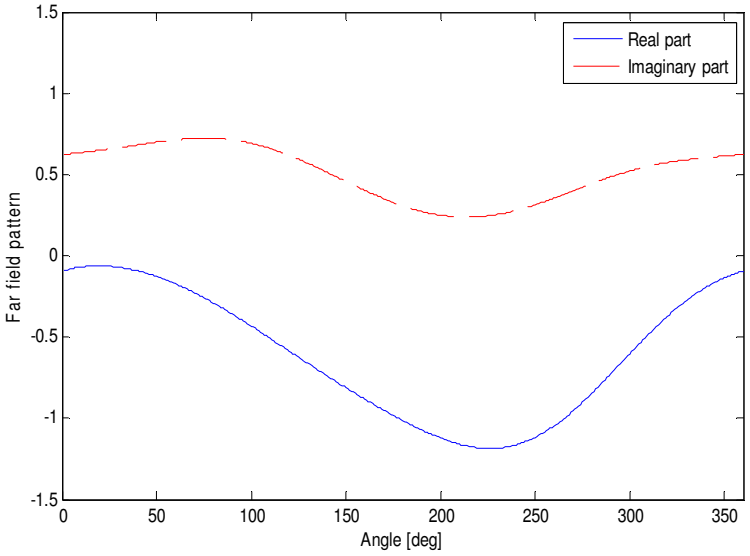

Figure 5.2 : Far field pattern of peanut shaped object for $d = (-1/\sqrt{2}, -1/\sqrt{2})$.

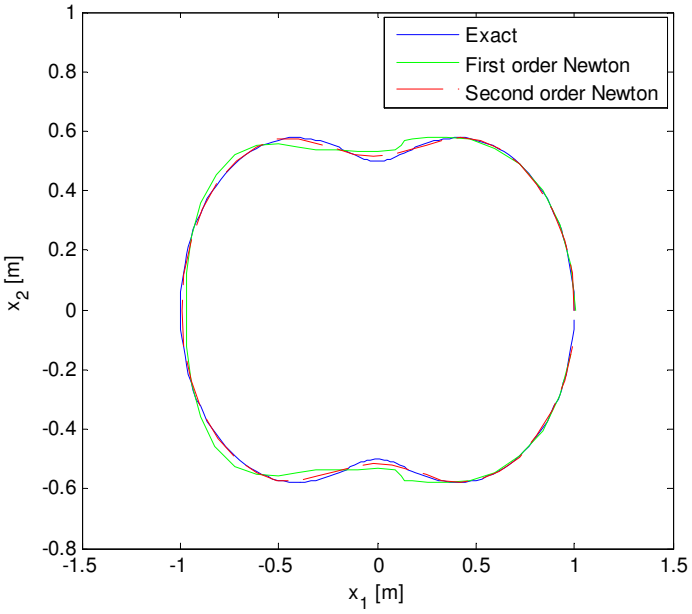

Figure 5.3 : Reconstruction of Peanut shaped object for $d = (-1,0)$ and exact data.

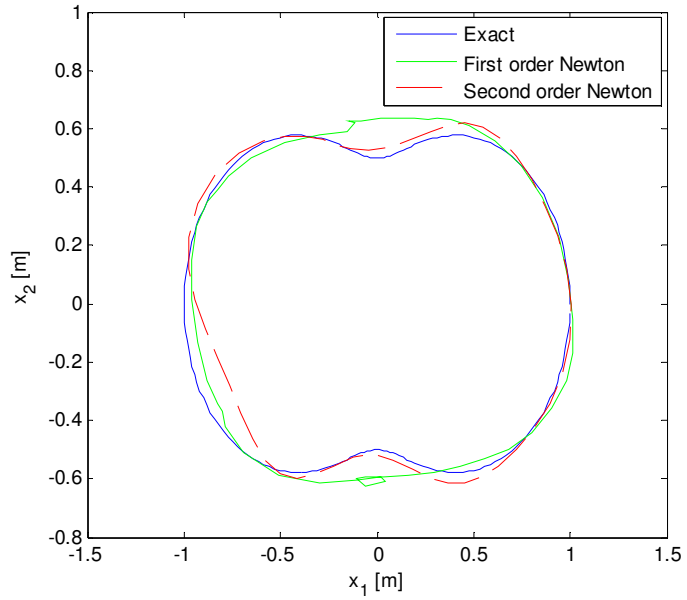

Figure 5.4: Reconstruction of Peanut shaped object for $d = (-1,0)$ and %3 noisy data.

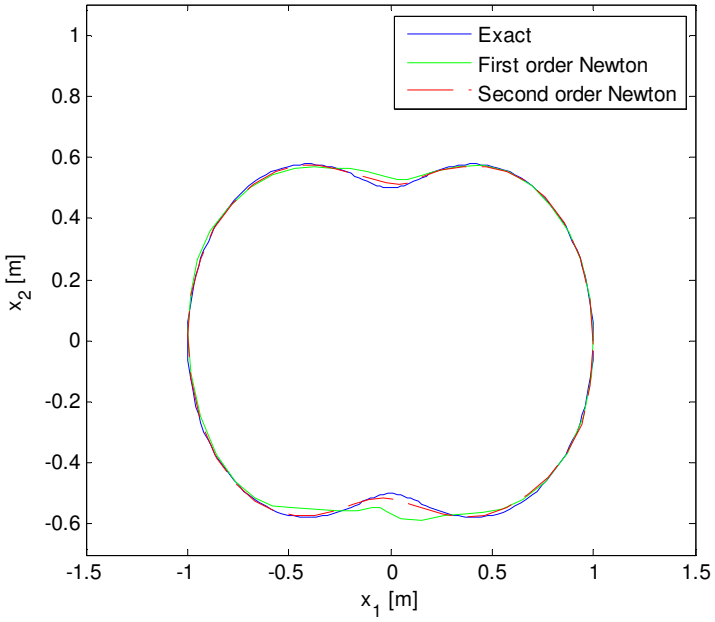

Figure 5.5 : Reconstruction of Peanut object for $d = (-1/\sqrt{2},-1/\sqrt{2})$ and exact data.

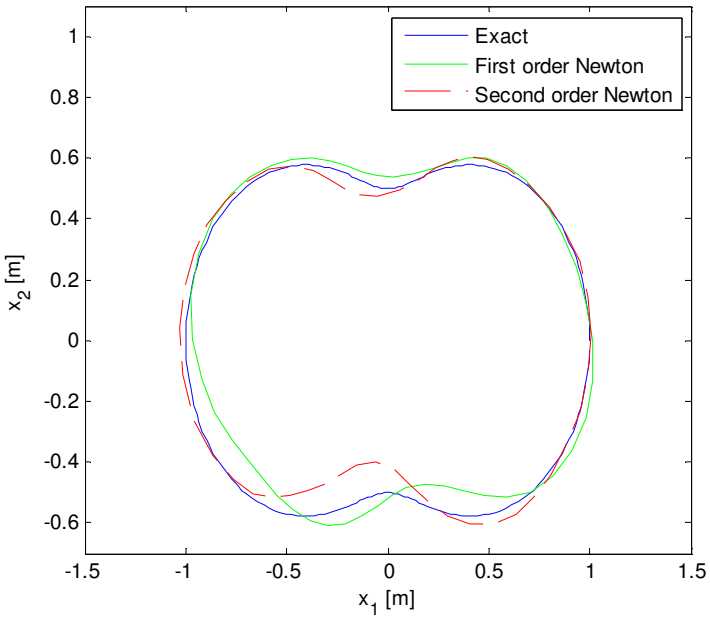

Figure 5.6 : Reconstruction of Peanut object for $d=(-1/\sqrt{2},-1/\sqrt{2})$ and %3 noisy data.

In the second example, we consider the identification of a kite-shaped object with the parameterization,

$$\partial D = \{ (\cos t + 0.65\cos t - 0.65, 1.5\sin t) : t \in [0,2\pi)\}\,[m] \qquad \textbf{(5.6)}$$

for two different angles of incidence. Iteration was started with a circle of radius 1.5m and poynomial degree $J = 9$ was selected. For the incident directions $d = (-1,0)$ and $d = (1,0)$ and for exact data, the change of the residual during the iterations are illustrated through Table 5.5 and Table 5.6 respectively and for noisy data, illustrated through Table 5.7 and Table 5.8 respectively. Far field patterns of kite shaped object for $d = (-1,0)$ and $d = (1,0)$ incident directions are depicted in fig.5.7 and fig.5.8 respectively.

Table 5.5 : Residuals of Kite shaped object for $d = (-1,0)$ and exact data.

Iteration number	First order Newton	Second order Newton
0 (initial estimate)	5.2744	5.2744
1	0.9737	1.1716
2	0.2100	0.0487
3	0.1247	--
4	0.1158	--

Table 5.6 : Residuals of Kite shaped object for $d = (1,0)$ and exact data.

Iteration number	First order Newton	Second order Newton
0 (initial estimate)	4.8715	4.8715
1	0.7954	1.5308
2	0.3872	0.0430
3	0.1486	--
4	0.0903	--

Table 5.7 : Residuals of Kite shaped object for $d = (-1,0)$ and %3 noisy data.

Iteration number	First order Newton	Second order Newton
0 (initial estimate)	3.0692	3.0692
1	1.1165	0.4633
2	0.3167	0.1318
3	0.2035	--
4	0.1831	--
5	0.1813	--

Table 5.8 : Residuals of Kite shaped object for $d = (1,0)$ and %3 noisy data.

Iteration number	First order Newton	Second order Newton
0 (initial estimate)	4.8349	4.8349
1	1.1324	0.8606
2	0.4182	0.3128
3	0.3297	--
4	0.3234	--

The reconstructions of kite shaped object for $d = (-1,0)$ incident direction and exact and %3 noisy data are given by figure 5.9 and figure 5.10 respectively The reconstructions of kite shaped object for $d = (1,0)$ incident direction exact and %3 noisy data are given by figure 5.11 and figure 5.12 respectively.

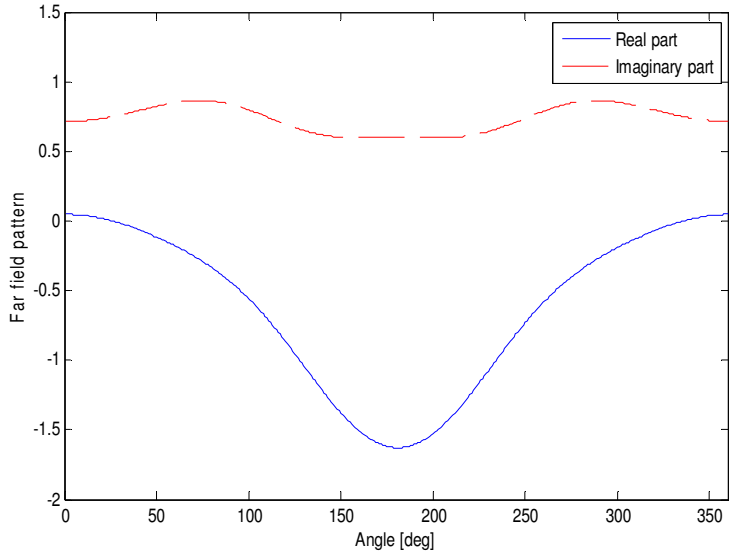

Figure 5.7 : Far field pattern of kite shaped object for $d = (-1,0)$ incident direction.

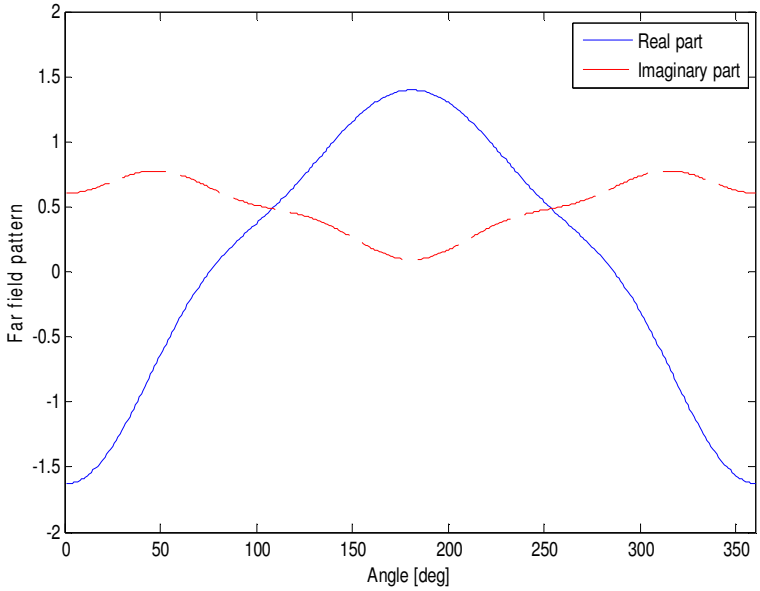

Figure 5.8 : Far field pattern of kite shaped object for $d = (1,0)$ incident direction.

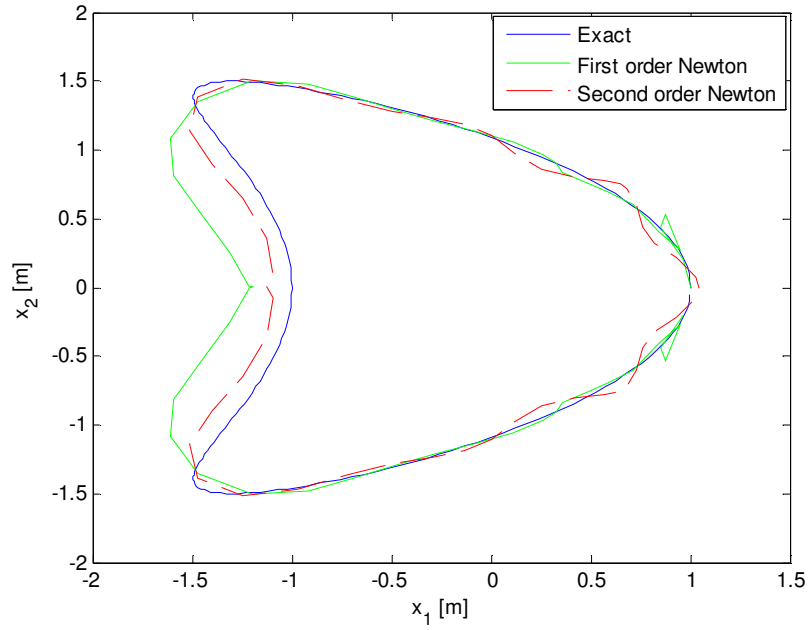

Figure 5.9 : Reconstruction of Kite shaped object for $d = (-1,0)$ and exact data.

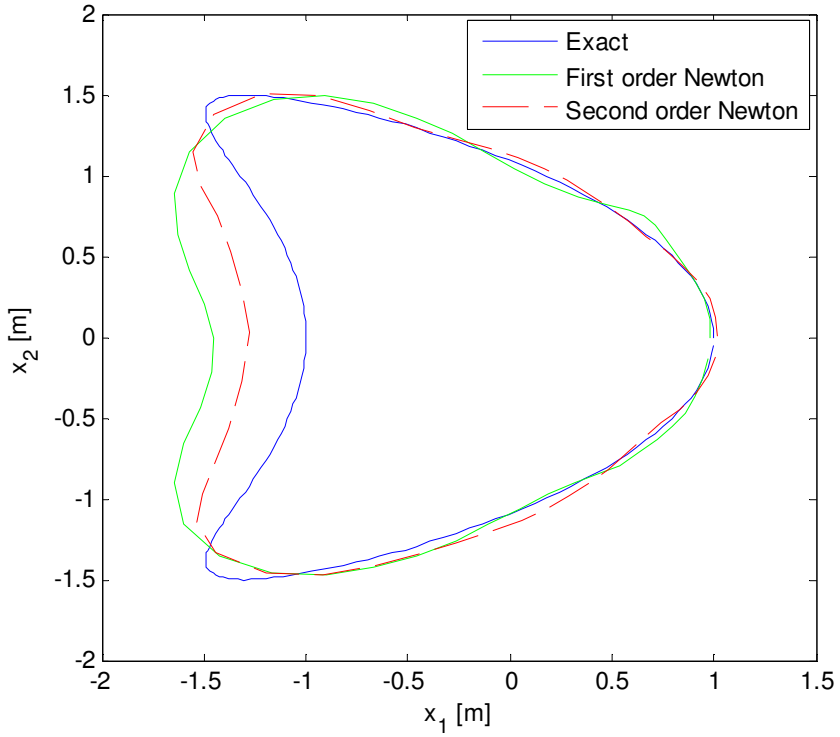

Figure 5.10: Reconstruction of Kite shaped object for $d = (-1,0)$ and $\%3$ noisy data.

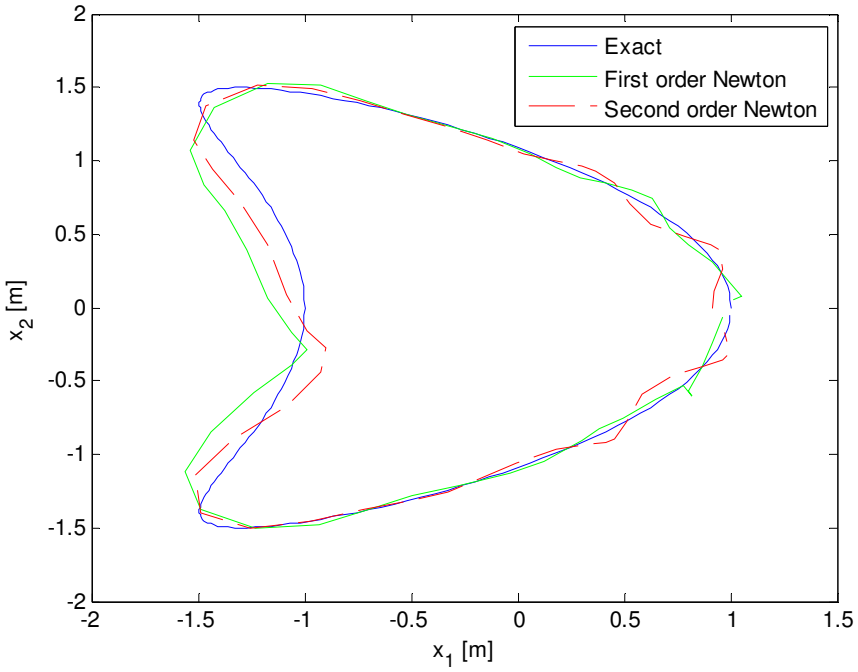

Figure 5.11 : Reconstruction of Kite shaped object for $d = (1, 0)$ and exact data.

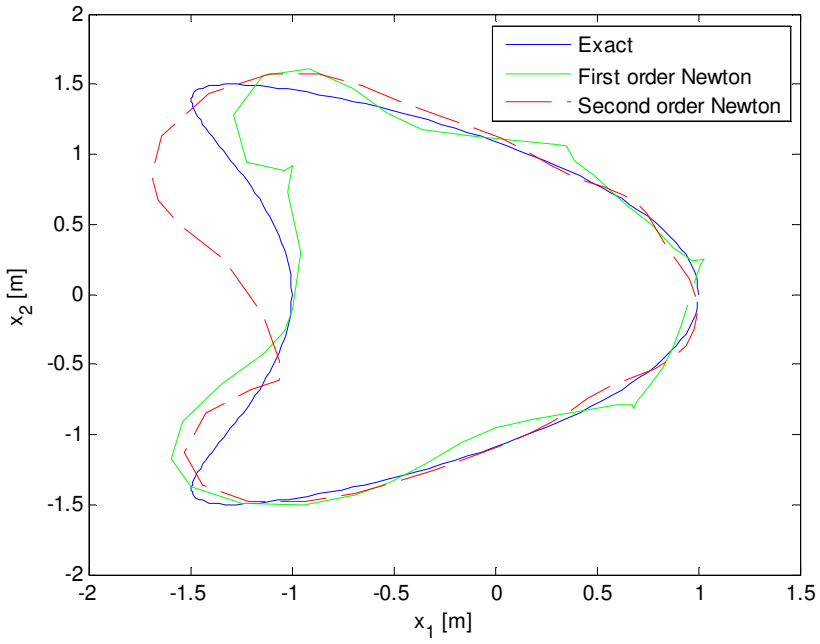

Figure 5.12 : Reconstruction of Kite shaped object for $d = (1, 0)$ and %3 noisy data.

In the third example, we consider the identification of an object with the parameterization given by,

$$\partial D = \{(2 + 0.3\cos(3t))\,(\cos t, \sin t) : t \in [0, 2\pi)\}\,[m] \qquad \textbf{(5.6)}$$

for incident directions $d = (-1,0)$ and $d = (-\sqrt{3}/2, -1/2)$. Far field patterns of object for $d = (-1,0)$ and $d = (-\sqrt{3}/2, -1/2)$ incident directions are depicted in fig.5.13 and fig.5.14 respectively. Iteration was started with a circle of radius 1m and poynomial degree $J = 6$ was selected. For the incident directions $d = (-1,0)$ and $d = (-\sqrt{3}/2, -1/2)$ and for exact data, the change of the residual during the iterations are illustrated through Table 5.9 and Table 5.10 respectively and for noisy data, illustrated through Table 5.11 and Table 5.12 respectively.

Table 5.9 : Residuals of the object for $d = (-1,0)$ and exact data.

Iteration number	First order Newton	Second order Newton
0 (initial estimate)	9.7291	9.7291
1	8.4913	5.0646
2	6.5985	1.1555
3	3.2368	0.3167
4	1.0412	0.0370
5	0.1956	--
6	0.0456	--

Table 5.10 : Residuals of the object for $d = (-\sqrt{3}/2, -1/2)$ and exact data.

Iteration number	First order Newton	Second order Newton
0 (initial estimate)	9.6817	9.6817
1	8.4888	2.4462
2	6.5367	0.5538
3	3.1243	0.1169
4	1.0579	0.0356
5	0.2132	--
6	0.0425	--

Table 5.11 : Residuals of the object for $d = (-1,0)$ and %3 noisy data.

Iteration number	First order Newton	Second order Newton
0 (initial estimate)	3.0692	3.0692
1	1.1165	0.4633
2	0.3167	0.1318
3	0.2035	--
4	0.1831	--
5	0.1813	--

Table 5.12 : Residuals of the object for $d = (-\sqrt{3}/2, -1/2)$ and %3 noisy data.

Iteration number	First order Newton	Second order Newton
0 (initial estimate)	9.5634	9.5634
1	7.4218	5.4220
2	2.3911	1.4691
3	1.9524	0.4686
4	1.7779	0.4575
5	1.6617	-
	1.5805	-

The reconstructions of object for $d = (-1,0)$ incident direction and exact and %3 noisy data are given by figure 5.15 and figure 5.16 respectively The reconstructions of peanut shaped object for $d = (-\sqrt{3}/2, -1/2)$ incident direction exact and %3 noisy data are given by figure 5.17 and figure 5.18 respectively.

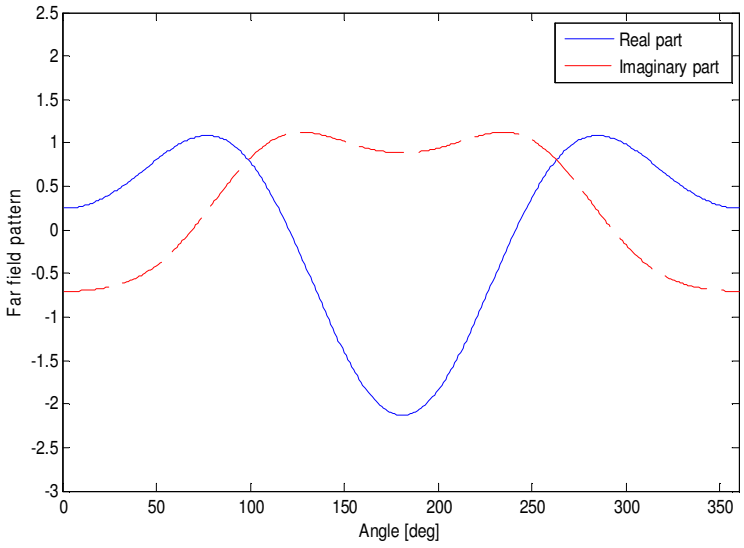

Figure 5.13 : Far field pattern of object for $d = (-1,0)$ incident direction.

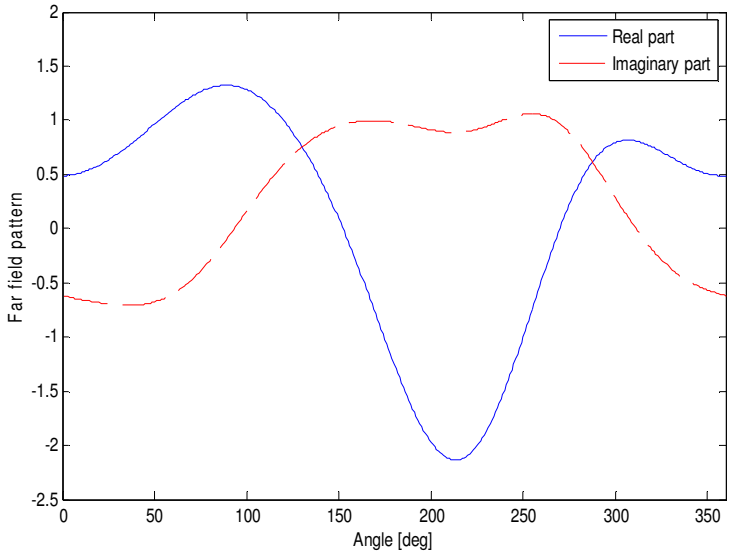

Figure 5.14 : Far field pattern of object for $d = (-\sqrt{3}/2, -1/2)$ incident direction.

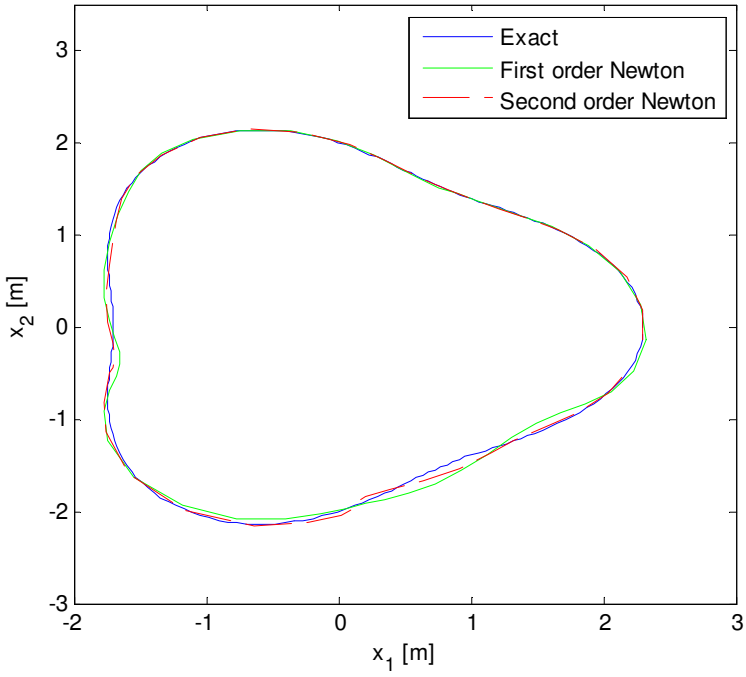

Figure 5.15 : Reconstruction of the object for $d = (-1, 0)$ and exact data.

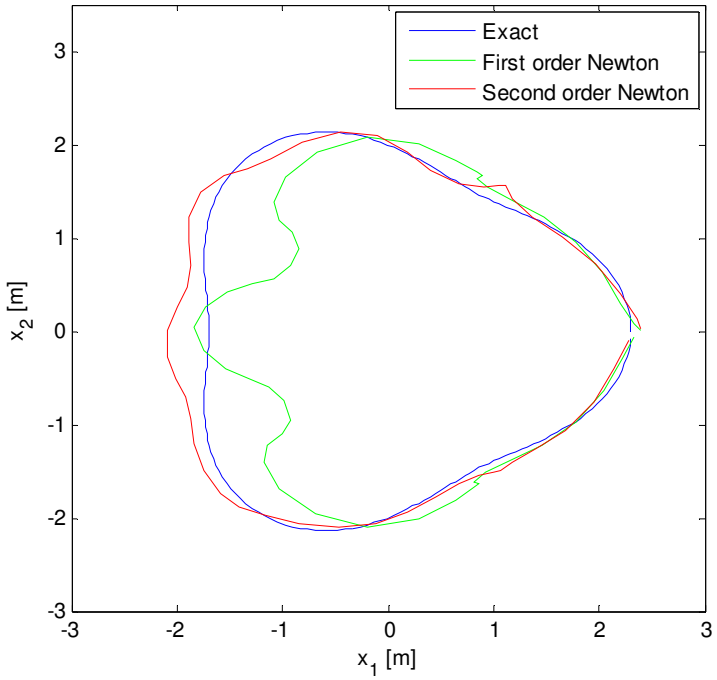

Figure 5.16 : Reconstruction of the object for $d = (-1,0)$ and %3 noisy data.

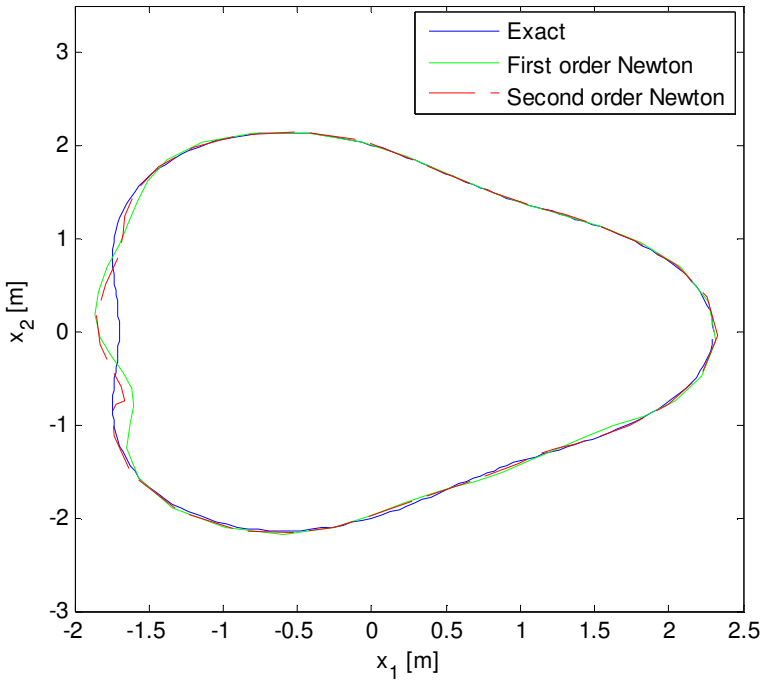

Figure 5.17 : Reconstruction of object for $d = (-\sqrt{3}/2, -1/2)$ and exact data.

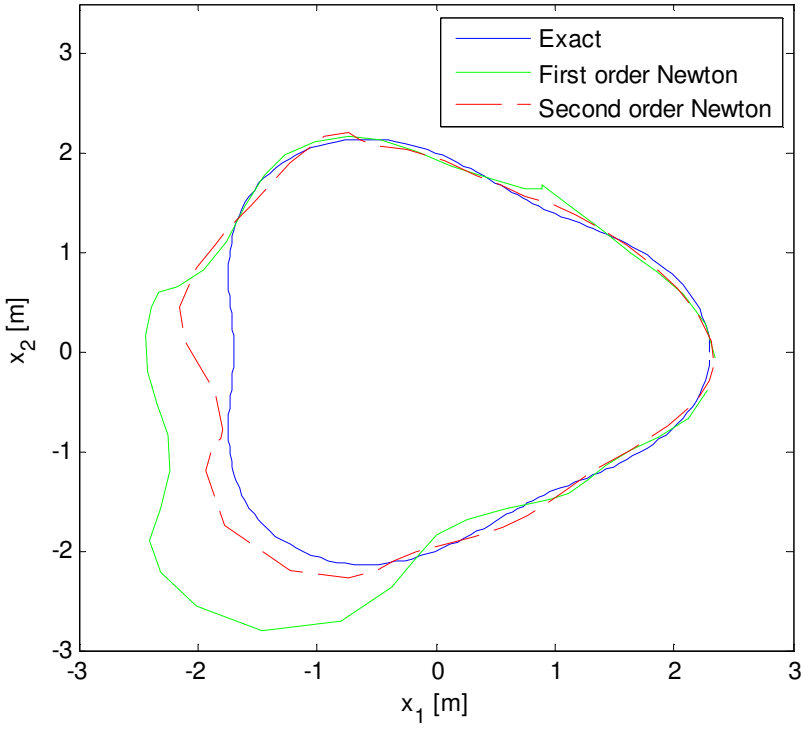

Figure 5.18 : Reconstruction of object for $d = (-\sqrt{3}/2, -1/2)$ and %3 noisy data.

In the fourth example, we consider the identification of square shaped object with edge 1.5m for incident directions $d = (-1,0)$. Far field pattern of square shaped object for $d = (-1,0)$ incident direction is depicted in fig.5.19. Iteration was started with a circle of radius 1m and poynomial degree $J = 6$ was selected. The change of the residual during the iterations are illustrated through Table 5.13 and Table 5.14 for exact and noisy data respectively. The reconstructions of square shaped object for $d = (-1, 0)$ incident direction and using exact and %3 noisy data are given by figure 5.20 and figure 5.21 respectively.

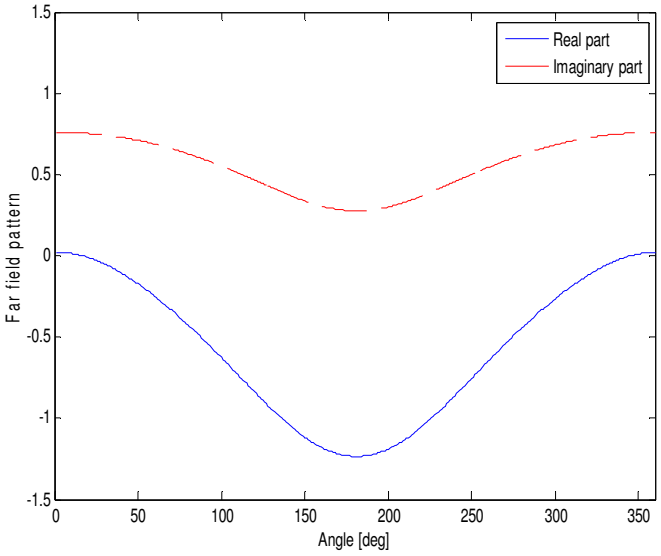

Figure 5.19 : Far field pattern of the square for $d = (-1,0)$ incident direction.

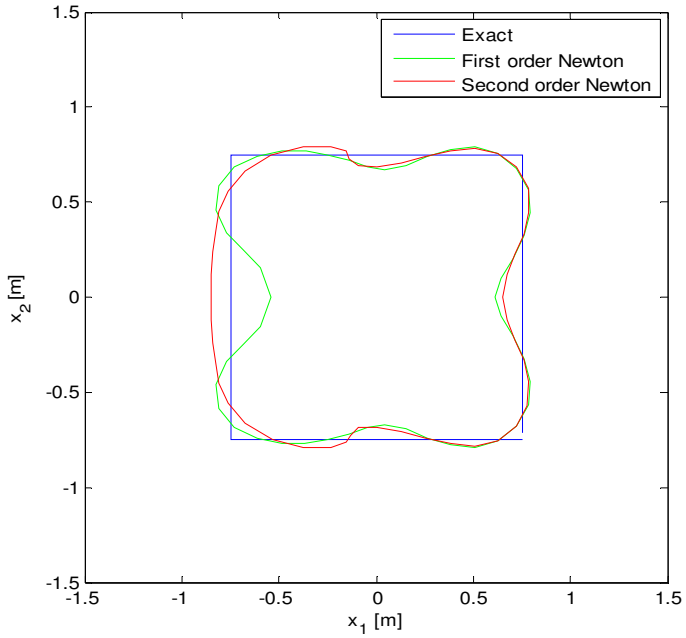

Figure 5.20 : Reconstruction of square for $d = (-1,0)$ and exact data.

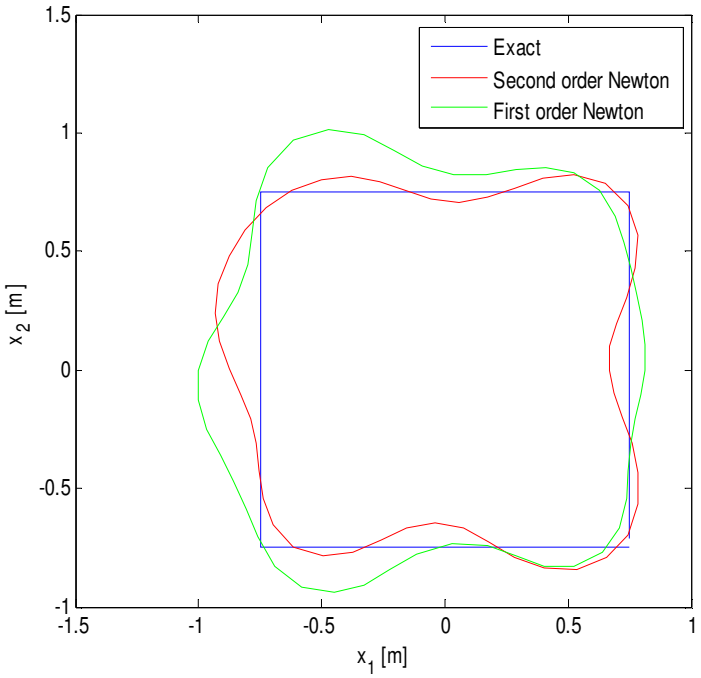

Figure 5.21 : Reconstruction of square for $d = (-1,0)$ and %3 noisy data.

Table 5.13 : Residuals of square for $d = (-1, 0)$ and exact data.

Iteration number	First order Newton	Second order Newton
0 (initial estimate)	1.1946	1.1946
1	0.3179	0.0801
2	0.1478	0.0192
3	0.0875	0.0147
4	0.0643	-
5	0.0543	-

Table 5.14 : Residuals of square for $d = (-1, 0)$ and %3 noisy data

Iteration number	First order Newton	Second order Newton
0 (initial estimate)	1.2118	1.2118
1	0.5426	0.1979
2	0.4528	0.1756
3	0.4478	-

6. CONCLUSIONS

We have presented a new second order method for solving the inverse obstacle scattering problem for PEC obstacles. Although there is a tremendous amount of competing algorithms and despite the lack of a rigorous convergence analysis, this method deserves attention due to its simple implementation and its reconstruction quality. Extension to other boundary conditions and to the three dimensional problem should be possible analogous to the corresponding first order method in [16, 17,18]. In addition, in principle, there is a straight forward extension to the case of limited angle data by modifying the far field equation appropriately, of course, at the cost of increasing the degree of ill-posedness. Furthermore, also the case of near field data can be accommodated through again modifying the data equation accordingly. This method decomposes the inverse scattering problem into ill-posed and non-linear part and deals with each part of the problem separately. This provides that method does not need forward solver in each iteration step. On the other hand, another advantage of this approach is that the cost functional of the nonlinear part of the problem has a particularly simple structure from which the first and second order Frechet derivatives are easily and analytically computed by exploiting the fact that field satisfies Heltmoltz equation outside the object [13]. This provides each iteration of second order and first order Newton needs approximately same CPU time. It is observed each iteration step requires 1.7083s and 1.7147s for the first and second order Newton methods respectively, if computer with 1800MHz clock frequency is used. Therefore, second order approach does not increase computational complexity. We obtained better reconstruction of illuminated region of the object than shadow region of the object. By means of multi-view illumination as given in section 3.3, it is possible to obtain better reconstructions especially in shadow region of the object. Proposed Newton reconstruction methods can be extended for reconstruction of perfectly electric conducting (PEC) objects located on known domain by using the fundamental solution of Helmholtz equation on known domain and its far field pattern and using the incident field as field in the absence of the PEC object. Fundamental solution of Helmoltz equation on known domain $\phi(x, y)$ simply is total

field on x if line source located on y. This is well known direct scattering problem. Therefore, $\phi(x, y)$ can be obtained straightforwardly. Field in the absence of the PEC object can also be obtained via direct scattering problem for plane wave excitation. Using these interchanging on section 3.1 and section 3.2, it is possible proposed Newton methods for reconstruction of PEC objects located in known domain. Particularly, reconstruction of object buried in an arbitrary shaped dielectric cylinder or buried in a half space are given in [23] and [24] respectively.

REFERENCES

[1] Roger, A., 1981: Newton Kantorovich algorithm applied to an electromagnetic inverse problem, *IEEE Trans. Ant. Prop.* AP-29, 232–238.

[2] Kirsch A., 1993**:** The domain derivative and two applications in inverse scattering, *Inverse Problems,* 9, 81–96**.**

[3] Potthast R., 1994: Frechet differentiability of boundary integral operators in inverse acoustic scattering, *Inverse Problems,* 10, 431–447.

[4] Colton, D. and Kress, R., 1998: *Inverse Acoustic and Electromagnetic Scattering Theory*. 2nd. ed. Springer, Berlin.

[5] Hettlich, F., 1995: Frechet derivatives in inverse obstacle scattering, *Inverse Problems*, 11, 371–382.

[6] Kress, R. and Paivarinta, L., 1999: On the far field in obstacle scattering, *SIAM J. Applied Math.*, 59, 1413–1426.

[7] Kirsch, A. and Kress, R., 1987: *An optimization method in inverse acoustic scattering, in Boundary Elements IX*, C. Brebbia, W. Wendland, and G. Kuhn, eds., Springer-Verlag, Heidelberg, 1987, pp. 3–18.

[8] Angell, T., Jiang, X. and Kleinman, R., 1997: On a numerical method for inverse acoustic scattering, *Inverse Problems,* 13, 531–545.

[9] Colton, D., Monk, P., 1987: The numerical solution of the three dimensional inverse scattering problem for time harmonic acoustic waves, *SIAM J. Sci. Stat. Comp.*, 8, 278–291.

[10] Misici, L. and Zirilli, F., 1994: Three dimensional inverse obstacle scattering for time harmonic acoustic waves: a numerical method, *SIAM J. Sci. Stat. Comp.*, 15, 1174–1189.

[11] Potthast, R., 1998: A point-source method for inverse acoustic and electromagnetic obstacle scattering problems, *IMA J. Applied. Math.*, 61 (1998), 119–140.

[12] Colton, D., Coyle, J., and Monk P., 2000: Recent developments in inverse acoustic scattering theory*, SIAM Review* 42, 369-414.

[13] R. Kress, N. S. Tezel, F. Yaman, A second order Newton method for sound soft inverse obstacle scattering, *Journal of Inverse and ill-posed Problems*, Vol. 17, Issue 2, 173-185, 2009.

[14] Kress, R., 2003: Newton's Method for inverse obstacle scattering meets the method of least squares, *Inverse Problems* 19, 91–104.

[15] Kress R. and Serranho P., 2005: A hybrid method for two-dimensional crack reconstruction, *Inverse Problems* 21, 773–784 .

[16] Kress R. and Serranho P., 2007: A hybrid method for sound-hard obstacle reconstruction, *J. Comput. Appl. Math.* 204, 418–427.

[17] Serranho, P., 2007: A hybrid method for inverse scattering for sound-soft obstacles in 3D., *Inverse Problems and Imaging* 1, 691–712.

[18] Serranho, P., 2006: A hybrid method for inverse scattering for shape and impedance, *Inverse Problems* 22, 663–680.

[19] Hettlich, F. and Rundell, W., 2000: A second degree method for nonlinear inverse problem, *SIAM J. Numer. Anal.* 37, 587–620.

[20] Cayören, M., Akduman, I., Yapar, A. and Crocco, L:, 2007: A new algorithm for the shape reconstruction of perfectly conducting objects. *Inverse Problems* 23,1087–1100

[21] Farhat, C., Tezaur, R., and Djellouli, R., 2002: On the solution of three-dimensional inverse obstacle acoustic scattering problems by a regularized Newton method, *Inverse Problems* 18, 1229–1246.

[22] Harbrecht, H. and Hohage, T., 2007: Fast methods for three-dimensional inverse obstacle scattering problems, *Jour. Integral Equations and Appl.* 19, 237–260.

[23] Tezel, N.S., Paker S., A second order Newton method for Reconstruction of PEC targets located in arbitrary shaped cylinder, *IEEE Transaction on Geoscience and Remote Sensing*. (submitted)

[24] Tezel, N.S., 2009: Newton's method for inverse obstacle scattering of buried objects, *Journal of Integral Equations and Applications*, Vol 21, Issue 3.

[25] Felsen, L. and Marcuvitz N., 1994: *Radiation and Scattering of Waves*, Wiley-IEEE Press.

[26] Altuncu Y., Yapar A., and Akduman I., 2007: Numerical computation of the Green's function of a layered media with rough interface" , *Microwave and Optical Technology Letters*, Vol.49 (5), 1204-1209, 2007

[27] Halley, E., 1694: A new, exact, and easy method of finding the roots of any equations generally, and that without any previous reduction, *Philos. Trans. Roy. Soc.* London 18, 136–148

[28] Hohage, T., 1997: Logarithmic convergence rates of the iteratively regularized Gauss- Newton method for an inverse potential and an inverse scattering problem, *Inverse Problems* 13, 1279–1299.

[29] Hohage, T., 1999: *Iterative Methods in Inverse Obstacle Scattering: Regularization Theory of Linear and Nonlinear Exponentially Ill-Posed Problems*, Dissertation, Linz.

[30] Potthast, R., 2001: On the convergence of a new Newton-type method in inverse scattering, *Inverse Problems* 17, 1419–1434.

[31] Deuflhard, P., Engl, H.W., and Scherzer, O., 1998: A convergence analysis of iterative methods for the solution of nonlinear ill-posed problems under affinely invariant conditions. *Inverse Problems* 14, 1081–1106.

[32] Engl, H.W., Hanke, M., and Neubauer, A., 1996: *Regularization of inverse problems*, Kluwer Academic Publisher, Dordrecht.

APPENDICES

APPENDIX A.1 : Expression of Second Order Normal Derivative of Field
APPENDIX A.2 : Numerical evaluation of the Green's function of domain containing arbitrary shaped dielectric cylinder
APPENDIX A.3 : Expression of the total field in the absence of the PEC object

APPENDIX A.1

Using the change of variables for the Laplace operator we have that

$$\Delta u(s,\varepsilon)=\frac{1}{\left|z'(t)+\varepsilon v'(t)\right|}\left\{\frac{\partial}{\partial s}\left(\frac{1}{\left|z'(s)+\varepsilon v'(t)\right|}\frac{\partial u}{\partial s}(s,\varepsilon)\right)+\frac{\partial}{\partial \varepsilon}\left(\left|z'(s)+\varepsilon v'(s)\right|\frac{\partial u}{\partial \varepsilon}(s,\varepsilon)\right)\right\} \quad \textbf{(A1.1)}$$

Therefore

$$\Delta u(s,0)=-\frac{z'(s).z''(s)}{\left|z'(s)\right|^4}\frac{\partial u}{\partial s}(s,0)+\frac{1}{\left|z'(s)\right|^2}\frac{\partial^2 u}{\partial s^2}(s,0)+\frac{z'(s).v'(s)}{\left|z'(s)\right|^2}\frac{\partial u}{\partial \varepsilon}(s,0)+\frac{\partial^2 u}{\partial s^2}(s,0) \quad \textbf{(A1.2)}$$

and observing that u satisfies the Helmholtz equation we find that

$$\frac{\partial^2 u}{\partial \varepsilon^2}(s,0)=-k^2u(s,0)+\frac{z'(s).z''(s)}{\left|z'(s)\right|^4}\frac{\partial u}{\partial s}(s,0)-\frac{1}{\left|z'(s)\right|^2}\frac{\partial^2 u}{\partial s^2}(s,0)-\frac{z'(s).v'(s)}{\left|z'(s)\right|^2}\frac{\partial u}{\partial \varepsilon}(s,0) \quad \textbf{(A2.2)}$$

APPENDIX A.2

Green's function of domain with arbitrary shaped dielectric cylinder $G(x, y)$ is the total field in the x if line source is located on y as depicted fig. A2.

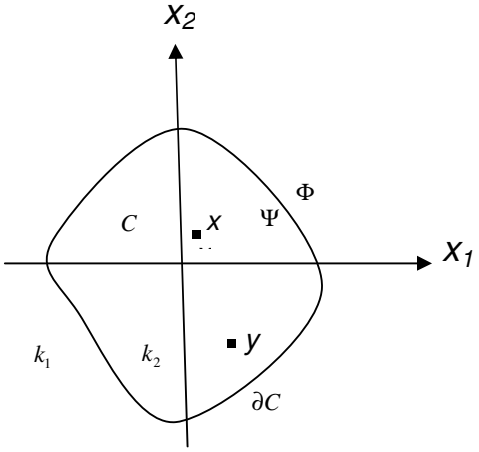

Figure A2: The domain whose Green's function has to be evaluated.

If a line source is located point y that is inside the dielectric cylinder, the total field outside and inside of the dielectric cylinder can be expressed respectively as [14],

$$u_1(x, y) = \int_{\partial C} \Phi(g, y) G_1(x, g) ds(g), \quad x \in R^2 \setminus C,\ y \in C \tag{A2.1}$$

$$u_2(x, y) = (i/4) H_0^{(1)}(k_2 |x - y|) + \int_{\partial C} \Psi(g, y) G_2(x, g) ds(g), \quad x \in C,\ y \in C \tag{A2.2}$$

where,

$$G_{1,2}(x, g) = \frac{i}{4} H_0^{(1)}(k_{1,2} |x - g|) \tag{A2.3}$$

As seen from (A2.1), (A2.2) and (4.8), u_1 and second term of u_2 correspond to $G_t(x, y)$ and $G_r(x, y)$ in (4.8) respectively. The total field has to satisfy boundary condition as,

$$\begin{aligned} &u_1(x) = u_2(x), \quad x \in \partial C \\ &\frac{\partial u_1(x)}{\partial v} = \frac{\partial u_2(x)}{\partial v}, \quad x \in \partial C \end{aligned} \tag{A2.4}$$

Substituting (A2.1) and (A2.2) into (A2.4) and using the jump relation of single layer potential, one gets integral equation as,

$$\int_{\partial C}\Phi(g,y)H_0^{(1)}(k_1|x-g|)ds(g)-\int_{\partial C}\Psi(g,y)H_0^{(1)}(k_2|x-g|)ds(g)=H_0^{(1)}(k_2|x-y|) \quad \textbf{(A2.5)}$$

$$\begin{aligned}\int_{\partial C}\Phi(g,y)\frac{\hat{v}(x)\{x-g\}}{|x-g|}k_1H_1^{(1)}(k_1|x-g|)ds(g)+(1/2)(\Phi(x,y)-\Psi(x,y))\\ -\int_{\partial C}\Psi(g,y)\frac{\hat{v}(x)\{x-g\}}{|x-g|}k_2H_1^{(1)}(k_2|x-g|)ds(g)=\frac{\hat{v}(x)\{x-y\}}{|x-y|}k_2H_1^{(1)}(k_2|x-y|)\end{aligned} \quad \textbf{(A2.6)}$$

For any location of the line source as *y*, one obtains two integral equations with two unknown as Φ and Ψ given by (A2.5) and (A2.6) which can be solved any numerical method such as method of moments (MoM) or Nyström [9].

Substitutions of Φ and Ψ into (A2.1) and (A2.2) respectively, one obtains the total field for line source excitation that is Green's function of the domain.

Far field pattern of the single layer potential φ on the boundary of the object Γ_0 can be expressed by (A2.1), (4.7) and using large argument approximation of Hankel functions as,

$$\begin{aligned}\frac{e^{ik_1|x|}}{\sqrt{|x|}}u_\infty(\hat{x})=\lim_{|x|\to\infty}\int_{\Gamma_0}\varphi(y)\int_{\partial C}\Phi(g,y)G_1(x,g)ds(g)ds(y)=\\ \frac{e^{i\pi/4}}{\sqrt{8\pi k_1}}\frac{e^{ik_1|x|}}{\sqrt{|x|}}\int_{\partial C}e^{-ik_1\hat{x}.g}\int_{\Gamma_0}\varphi(y)\Phi(g,y)ds(y)ds(g)\end{aligned} \quad \textbf{(A2.7)}$$

that gives (4.9).

APPENDIX A.3

Total field in the absence of the PEC object can be expressed by similar procedure as Appendix A. For the plane wave excitation, total field inside and outside of the cylinder can be given respectively as,

$$u_1(x) = e^{ik_1 x.\hat{k}_i} + \int_{\partial C} \Psi(y) G_1(x,y) ds(y), \quad x \in R^2 \setminus C \tag{A3.1}$$

$$u_2(x) = \int_{\partial C} \Phi(y) G_2(x,y) ds(y), \quad x \in C \tag{A3.2}$$

where $\hat{k}_i = (-\cos\phi_0, -\sin\phi_0)$ is incident direction of plane wave. The total field has to satisfy boundary condition as,

$$\begin{aligned} &u_1(x) = u_2(x) \\ &\frac{\partial u_1(x)}{\partial v} = \frac{\partial u_2(x)}{\partial v} \end{aligned} \tag{A3.3}$$

Substituting (A3.1) and (A3.2) into (A3.3), one gets two integral equations as

$$\int_{\partial C} \Phi(y) H_0^{(1)}(k_1|x-y|) ds(y) - \int_{\partial C} \Psi(y) H_0^{(1)}(k_2|x-y|) ds(y) = e^{ik_1 x.\hat{k}_i} \tag{A3.4}$$

$$\begin{aligned} &\int_{\partial C} \Phi(y) \frac{\hat{v}(x)\{x-y\}}{|x-y|} k_1 H_1^{(1)}(k_1|x-y|) ds(y) + (1/2)(\Phi(x) - \Psi(x)) \\ &\quad - \int_{\partial C} \Psi(y) \frac{\hat{v}(x)\{x-y\}}{|x-y|} k_2 H_1^{(1)}(k_2|x-y|) ds(y) = -ik_1 \hat{v}(x) \hat{k}_i e^{ik_1 x.\hat{k}_i} \end{aligned} \tag{A3.5}$$

with two unknown Φ, Ψ that can be solved straightforwardly. Substituting Φ into (A3.2) gives the total field inside of the cylinder in the absence of PEC object.

CURRICULUM VITA

Candidate's full name: Necmi Serkan Tezel

Place and date of birth: Edremit, 1978

Permanent Address: Istanbul Technical University (I.T.U) Electronics and Communication Department, 34469, Maslak Istanbul/ Turkey

Universities and Colleges attended:

1999-2001 MsC: I.T.U – Institute of Science and Technology
Electronics and Communication Department
1994-1999 BsC I.T.U. – Electrical and Electronics Faculty,
Electronics and Communication Department
1987-1994 Edremit College

Publications:

- Necmi Serkan Tezel, Selçuk Paker, Electromagnetic scattering by arbitrary shaped inhomogeneous impedance cylinder using physical optics method, Microwave and Optical Technology Letters, Volume 48, Issue 7, 2006.
- Necmi Serkan Tezel, Selçuk Paker, Electromagnetic scattering from cylinder described by high-order inhomogeneous impedance boundary conditions, Microwave and Optical Technology Letters, Volume 48, Issue 6, 2006.
- Serkan Şimşek, Cevdet Işık, Necmi Serkan Tezel, İnci Akkaya, 'Expressions of radiation field and input resonance resistance of coaxial and microstrip line fed rectangular microstrip antennas' Microwave and Optical Technology Letters Volume 49, Issue 4, Date: April 2007, Pages: 817-822.

- Necmi Serkan Tezel, Serkan Şimşek, Neural Network Approach to Shape Reconstruction of a Conducting Cylinder, Istanbul University Journal of Electrical & Electronics Engineering, Volume 7, Number 1, pp. 299-304, 2007.

- Necmi Serkan Tezel, Serkan Simsek, Bayram Esen, Calculation of the Scattering Fields for Impedance Sphere by Using Series Expansion Method, Istanbul University Journal of Electrical & Electronics Engineering, Volume 3, Number 2, pages 927-933, 2003.

- Necmi Serkan Tezel, 'Electromagnetic scattering from high order inhomogeneous impedance cylinder of arbitrary shape by using physical optics' Microwave and Optical Technology Letters Volume 49, Issue 5, Date: May 2007, Pages: 1031-1036.

- Necmi Serkan Tezel, 'Electromagnetic scattering from cylinder with generalized impedance boundary condition' Microwave and Optical Technology Letters Volume 49, Issue 12, Date: December 2007, Pages: 3090-3093.

- Necmi Serkan Tezel, 'Electromagnetic Scattering from Perfectly Conducting Periodic Surfaces by Transforming into Equivalent Boundary Condition' Microwave and Optical Technology Letters, Volume 50, Issue 8, August 2008, Pages: 1997-2000

- Necmi Serkan Tezel, 'A new formulation and solution method of electromagnetic scattering from arbitrary shaped dielectric objects' Microwave and Optical Technology Letters, Volume 50, Issue 11, Date: November 2008, Pages: 2768-2772.

- Necmi Serkan Tezel, 'Electromagnetic Scattering from Anisotropic Inhomogeneous Impedance Cylinder of Arbitrary Shape by Physical Optics' IEEE Geoscience and Remote Sensing Letters, Vol. 5, Issue 4, pages 663-667, 2008.

- R. Kress, N. S. Tezel, F. Yaman, 'A second order Newton method for sound soft inverse obstacle scattering.' Journal of Inverse and ill-posed Problems, Vol. 17, Issue 2, 173-185, 2009.

- Necmi Serkan Tezel, 'Newton's method for inverse obstacle scattering of buried objects' Journal of Integral Equations and Applications' Journal of Integral Equations and Applications, Vol 21, Issue 3, 2009

- Necmi Serkan Tezel, 'Hybrid method for shape reconstruction of dielectric objects', Microwave and Optical technology Letters, Vol 51, Issue 4, p. 1147-1151 April 2009.

- Necmi Serkan Tezel, N. Gökhan Kasapoğlu, Bingül Yazgan ' *Velocity İmaging System for Detection of Moving Targets'* , International Conference on Electrical and Electronics Engineering 7-11 November Bursa, Turkey (ELECO 2001)

- N. Gökhan Kasapoğlu, Necmi Serkan Tezel, Bingül Yazgan ' *Sar Raw Data Compression with DCT-BAQ'* , International Conference on Electrical and Electronics Engineering 7-11 November Bursa, Turkey (ELECO 2001).

- Necmi Serkan Tezel, Selçuk Paker, Bingül Yazgan '*Linear Receiving System for Detection of Moving Targets'* 4th European Conference on Synthetic Aperture Radar pp. 649-653, 4-6 June 2002, Cologne ,Germany.

- Serkan Simsek, Necmi Serkan Tezel, Inci Akkaya *'Calculation of Radiation Field and Input Impedance of Rectangular Microstrip Antenna by New Method'* URSI 2002 Bilimsel Kongresi ve Ulusal Genel Kurul Toplantisi sf. 58-63 18-20 Eylül 2002, Istanbul Teknik Üniversitesi, Istanbul. Türkiye.

▪ Necmi Serkan Tezel *'Comparasion of Radiation Pattern of Array Antenna fed by different Tapering Functions'* URSI 2002 Bilimsel Kongresi ve Ulusal Genel Kurul Toplantisi sa. 131-134 18-20 Eylül Istanbul Teknik Üniversitesi, Istanbul. Türkiye.

▪ Serkan Simsek, Necmi Serkan Tezel, Inci Akkaya *'Expression of Input Impedance and Radiation Field of Circular Microstrip Antenna by New Method '*, ELECO'2002, sf.132-135,18-22 Aralik 2002.

▪ Necmi Serkan Tezel, Ali Yapar, Selçuk Paker *' Coupling Effects of the Impedance Cylinder Located Between the Parallel Lines '* The 2003 IEEE International Symposium on Electromagnetic Compatibility (EMC2003) 11-16 May 2003 Istanbul Hilton, Istanbul,Turkey.

▪ Necmi Serkan Tezel, Serkan Simsek *' Evaluation of the Scattering Matrix for Impedance Sphere '* The 2003 IEEE International Symposium on Electromagnetic Compatibility (EMC2003) 11-16 May 2003 Istanbul Hilton, Istanbul,Turkey.

▪ Necmi Serkan Tezel, Isa Yildirim *'Inverse Synthetic Aperture Radar Imaging for Point Scatterers Using APES Algorithm'* International Conference on Electrical and Electronics Engineering 7-11 November Bursa, Turkey, 3-7 Aralik 2003.

▪ Isa Yildirim, **Necmi Serkan Tezel** *' Simulation of Synthetic Aperture Radar Imaging Using Capon Spectrum Estimation Method '* International Conference on Electrical and Electronics Engineering 7-11 November Bursa, Turkey (ELECO 2003)., 3-7 Aralik 2003.

▪ **Necmi Serkan Tezel,** Serkan Simsek *' Minimization of Jamming Effects for Planar Array Antennas by Using Adaptive Side Lobe Reduction Method in Space Domain'* International Conference on Electrical and Electronics Engineering 7-11 November Bursa, Turkey (ELECO 2003).3-7 Aralik 2003

▪ Isa Yildirim**, Necmi Serkan Tezel,** Isin Erer, Bingül Yazgan *' Comprasion of Non-parametric Spectral Estimators for SAR Imaging '* International Conference on Recent Advances in Space Technologies (RAST 2003) 20-22 Nov. 2003 Istanbul, Turkey.

▪ **Necmi Serkan Tezel,** Selçuk Paker *' Investigation and Reduction of Noise Jamming Effects on SAR Imaging System '* European Conference on Synthetic Aperture Radar 25-27 May 2004, Ulm, Germany.

▪ Isa Yildirim, **Necmi Serkan Tezel** *' Adaptive Finite Impulse Response Filtering for SAR Imaging'* European Conference on Synthetic Aperture Radar 25-27 May 2004, Ulm, Germany.

▪ Necmi Serkan Tezel, Selcuk Paker *' Minimization of Mono-static Radar Cross Section of Impedance Cylinder by Changing Surface Impedance Distribution'* URSİ 2004, 8-10 Eylül 2004 Bilkent Ankara, Türkiye.

▪ Necmi Serkan Tezel, Serkan Simsek *'Interference Reduction by Adaptive Weighting Using Steepest Descent Method for Any Array Configuration' ,* IEEE AP-S International Symposium and USNC-URSI Meeting, 3-8 July 2005, Washington, D.C. U.S.A.

▪ Necmi Serkan Tezel, Selçuk Paker 'Bi-Static Scattering Width Control of Multiple Coated PEC Cylinder' , IEEE International Geoscience andRemote Sensing Symposium 25-29 July 2005, Seoul, Korea.

- Necmi Serkan Tezel, Selçuk Paker ‘ *Inserting moving targets by Jamming into SAR image’* 6th European Conference on Synthetic Aperture Radar 16-18 May 2006, Dresten, Germany

- Necmi Serkan Tezel, Selçuk Paker ‘ *Bi-static Radar Cross Section Reduction of Impedance Cylinder*’ 2006 IEEE Radar Conference, 24-27 April 2006, Verona, New York, USA.